

Early processing of Bid and caspase-6, -8, -10, -14 in the canine brain during cardiac arrest and resuscitation[☆]

Maryla Krajewska,^{a,1} Robert E. Rosenthal,^{b,1} Jowita Mikolajczyk,^a Henning R. Stennicke,^{a,c} Thomas Wiesenthal,^a Juergen Mai,^{a,d} Mikihiro Naito,^e Guy S. Salvesen,^a John C. Reed,^a Gary Fiskum,^{f,*} and Stan Krajewski^{a,*}

^aThe Burnham Institute, La Jolla, CA 92037, USA

^bProgram in Trauma, Department of Surgery, University of Maryland School of Medicine, Baltimore, MD 21201, USA

^cDepartment of Protein Design, Protein Chemistry, Discovery, Novo Nordisk A/S, DK-2880 Bagsvaerd, Denmark

^dDepartment of Anatomy, H-Heine University of Duesseldorf, Duesseldorf, Germany

^eInstitute of Molecular and Cellular Biosciences, University of Tokyo, Tokyo, Japan

^fDepartment of Anesthesiology, University of Maryland School of Medicine, Baltimore, MD 21201, USA

Received 31 October 2003; revised 8 April 2004; accepted 5 May 2004

Available online 20 July 2004

Abstract

A clinically relevant model of transient global brain ischemia involving cardiac arrest followed by resuscitation in dogs was utilized to study the expression and proteolytic processing of apoptosis-regulatory proteins. In the hippocampus, an increase in pro-apoptotic Bcl-2 family proteins Bcl-X_S and Bak was detected, concomitant with proteolysis of Bcl-X_L and Bcl-2, following ischemia–reperfusion injury. Also, biphasic cleavage of Bid was found in this region of the brain, with early generation of tBid-p11 within 10 min of cardiac arrest, followed by generation of tBid-p15 within 30-min reperfusion, consistent with activation of this pro-apoptotic protein. In addition, cardiac arrest and resuscitation induced early, reperfusion-dependent proteolytic processing of pro-caspase-6, -8, -10, and -14, which preceded caspase-3 activation. Immunohistochemical analysis using antibodies, which preferentially recognize processed caspase-3, -6, -8, and -10, provided evidence of time-dependent activation of these proteases in both neurons and glia in ischemia-sensitive regions of the brain.

In conclusion, extremely rapid, cell-selective processing of apoptosis-regulatory proteins occurs in a clinically relevant model of ischemic brain injury caused by cardiac arrest and resuscitation. The early cleavage of Bid and rapid depletion of 32-kDa pro-caspase-14 from the canine hippocampus after induction of ischemia suggests the involvement of calpains in the processing of these proteins. Demonstration of *in vitro* cleavage of recombinant mouse caspase-14 by calpain I in the present study lends support to this hypothesis, further implicating cross-talk between different protease families in the pathophysiology of ischemic neural cell death.

© 2004 Elsevier Inc. All rights reserved.

Keywords: Global brain ischemia; Bcl-2; Bid; Caspase-6, -8, -10, -14; Apoptosis; Necrosis

Introduction

Both apoptosis and necrosis contribute to the cell death that occurs in the brain following transient global or focal ischemia (Linnik et al., 1993; Snider et al., 1999). Deli-

neating the relative contributions of apoptosis and necrosis to neuronal death after ischemia has an important therapeutic relevance. However, increasing evidence indicates that these two forms of cell demise represent only the extreme ends of a continuum. (Nicotera et al., 1999).

Bcl-2-family proteins and caspase-family cell death proteases represent core components of the apoptotic machinery (Nicholson and Thornberry, 1997). At least 14 different caspase proteases have been identified in mammals (Nunez et al., 1998). From a functional perspective, these proteases have been classified into upstream “initiator” large prodomain caspases that act as signal transducers and downstream “effector” caspases containing

[☆] This work is dedicated to the memory of Prof. M.J. Mossakowski.

* Corresponding authors. Stan Krajewski is to be contacted at Fax: +1-858-646-3194, The Burnham Institute, La Jolla, CA 92037 and Gary Fiskum at Fax: +1-410-706-2550, Program in Neuroscience, University of Maryland School of Medicine, Baltimore, MD 21201.

E-mail addresses: stan@burnham.org (S. Krajewski), gfk001@umaryland.edu (G. Fiskum).

¹ Both authors contributed equally to the work presented.

only short N-terminal prodomains (Salvesen and Dixit, 1997).

At least two major pathways of caspase activation have been identified. One pathway is triggered by TNF-family receptors that recruit several intracellular proteins to their cytosolic domains, forming a “death-inducing signaling complex” (DISC) that triggers caspase-8 and -10 activation and leads to apoptosis (Yuan, 1997).

Another major apoptosis pathway centers on mitochondria, which release cytochrome *c* into the cytosol following a variety of cell death stimuli. Cytochrome *c* binds to the caspase activator, Apaf1, which then associates with and activates pro-caspase-9 (Green and Reed, 1998). The initiator caspases activated via these two pathways are capable of cleaving and activating directly or indirectly downstream effector caspases such as caspase-3, -6, and -7, thus propagating a cascade of proteolysis that results in apoptosis.

Additionally, alternative pathways involving cross-talk among other cell protease systems during ischemia have been proposed. Among these is calpain-induced cathepsin release (Yamashima et al., 1996), cathepsin-mediated caspase activation (Ishisaka et al., 1998), and caspase-mediated calpastatin degradation leading to sustained calpain activation, an event that may play a role in the ischemic neuronal death.

The Bcl-2-family proteins play crucial roles in the transduction of intracellular apoptotic signals in the nervous system. This gene family is composed of anti-apoptotic members such as Bcl-2, Bcl-X_L, Bcl-w, Mcl-1, Bfl-1, and Bcl-B and pro-apoptotic proteins which include Bax, Bak, Bad, Bok, Bik, Bid, Bim, Hrk, Blk, Bcl-X_S, Bnip3, Nix, Noxa, Bcl-G_S, PUMA, and Bmf. One of the features of Bcl-2 family proteins is the formation of homo- and heterodimers, whose relative abundance coincides with either cell death or survival (Reed, 1997).

Bcl-2-family proteins regulate the mitochondrial pathway for caspase activation by controlling cytochrome *c* release. Binding of Bid to Bax or Bak promotes their insertion into and oligomerization in membranes, forming pores through which molecules such as cytochrome *c*, SMAC, and Omi can escape from mitochondria (Korsmeyer et al., 2000). Conversely, anti-apoptotic proteins such as Bcl-2 and Bcl-X_L are well known for their ability to prevent cytochrome *c* release from mitochondria (Kluck et al., 1997; Yang et al., 1997).

The function of some Bcl-2-family proteins is regulated in part by caspases. For example, the anti-apoptotic Bcl-2 and Bcl-X_L proteins are converted into pro-apoptotic factors when cleaved by caspases (Bellows et al., 2000; Cheng et al., 1997). Cleavage of Bid by caspase-8 following Fas/TNR-R1 activation (Li et al., 1998) results in its activation and subsequent translocation to mitochondria, where it promotes apoptosis. These caspase-mediated effects on Bcl-2-family proteins define a pathway for connecting the death receptor and mitochondrial pathways for apoptosis.

Though some of the changes in expression and processing of caspases and Bcl-2-family proteins have been studied in rodent models of focal and global cerebral ischemia (Antonawich et al., 1998; Asahi et al., 1997; Cao et al., 2001; Gillardon et al., 1996b; Isenmann et al., 1998; Krajewski et al., 1995; Krupinski et al., 2000), it has never been investigated whether similar events occur in higher mammals. Demonstration of specific cell death pathways in large as well as small animal models of ischemic brain injury is important for eventual translation to neuroprotective intervention with human patients.

We previously utilized a clinically relevant canine cardiac arrest model of global cerebral ischemia to demonstrate the release of mitochondrial pro-caspase-9 into the cytosol of hippocampal and cortical neurons following cerebral ischemia–reperfusion injury (Krajewski et al., 1999). Using the same large animal model (Liu et al., 1998), we have now characterized the spatial and temporal patterns of expression and proteolytic processing of caspase and Bcl-2-family proteins.

Materials and methods

Animal experiments

All animal experiments were performed in accordance with the guidelines of the Institutional Animal Use and Care Committees of the University of Maryland, Baltimore, and the George Washington University. We employed a canine model of cardiac arrest and resuscitation as a clinically relevant large animal model for global cerebral ischemia and reperfusion, as described (Liu et al., 1998; Rosenthal et al., 1987, 2003). Six sham-controls and twenty-one adult female beagles were submitted to cardiac arrest experimentation (total 27). The animals weighing 10–15 kg were anesthetized with 15 mg/kg sodium pentothal, and prolonged anesthesia was induced by infusion of α -chloralose (75 mg/kg). Animals were endotracheally intubated and ventilated with room air before induction of cardiac arrest. Before arrest, muscle paralysis was maintained with intravenous pancuronium bromide. Following resuscitation, paralysis was used as needed to prevent fighting the ventilator, but only after assurance that adequate sedation was provided. Antibiotic prophylaxis was achieved with ceftriaxone. Resuscitative drugs were administered via venous catheter advanced to the level of the right atrium. Arterial pressure was continuously monitored through a femoral arterial catheter. Pulse, ECG, and rectal temperature were also continuously monitored and the temperature maintained between 37°C and 39°C by use of warming lights and heating blankets.

A left lateral thoracotomy was performed on all animals, including non-arrested controls. Ventricular fibrillation cardiac arrest was induced with a train of electrical current applied directly to the epicardium of the right ventricle

following incision and reflection of the pericardium. Artificial respiration was discontinued at the onset of fibrillation. Following 10 min of cardiac arrest, animals were either sacrificed or cardiopulmonary resuscitation (CPR) was initiated to allow for reperfusion periods of 30 min, 2, 4, 24, or 48 h. Resuscitation was initiated by open chest cardiac massage at the rate of 60/min, administration of epinephrine and sodium bicarbonate, and ventilation initially with 100% O₂. Open chest CPR was continued for 3 min followed by internal defibrillation. Arterial blood gas samples were measured before arrest, 2 min following defibrillation, and frequently thereafter. The ventilator was adjusted following the first blood gas determination and thereafter to maintain arterial pO₂ between 80 and 100 mm Hg and pCO₂ between 25 and 35 mm Hg. Artificial ventilation was maintained for 22 h, at which time the dogs were weaned from controlled ventilation. Animals were maintained under constant intensive care for up to 48 h. Postoperative pain was controlled using a constant infusion of morphine sulfate at 1 mg/h, with additional boluses administered as warranted.

Tissue acquisition

For immunohistochemistry, 18 dogs were perfused transcardially with ice-cold 1% paraformaldehyde in phosphate-buffered saline (PBS, pH 7.4) for 5 min followed by cold 4% paraformaldehyde in PBS for 15 min at a flow rate of 300 ml/min as previously described (Hof et al., 1996). After perfusion, the brains were immediately removed from the skull and postfixed in Bouin's solution (Sigma, Inc. St. Louis, USA), then embedded in paraffin.

For immunoblot analyses, the hippocampi of three sham-controls and six dogs after cardiac arrest (total nine) were removed from chloralose-anesthetized animals following a craniotomy and immediately before euthanasia with 0.25 ml/kg Euthanasia-6 (Veterinary Labs, Lenexa, KS). The surgeon excised the entire proximal region encompassing CA1–CA2 sectors. While the proximal portion of the hippocampus used for immunoblot analysis was similar for all animals, these samples may have contained a small portion of the CA3 sector in addition to the CA1–CA2 sectors. Before freezing in liquid nitrogen, each hippocampal sample was divided in half for duplicate lysate sample preparation. This intraoperative procedure and rapid freezing minimizes post-mortem alterations and allows for a precise control of the timing of sample harvesting after cardiac arrest.

Antibodies

The preparation and characterization of antibodies specific for Bcl-2 (AR-01, AR-08, and AR-09), Bcl-X (AR-04 specific for the long form and AR-05 recognizing Bcl-X-short), Bax (AR-10), Bak (AR-06), and Bid (AR52–54) have been described previously (Krajewski et al., 1994a, 1994c, 1995, 1996a, 2002b). A polyclonal antibody to caspase-3 (AR-14) was raised in rabbits using recombinant

human caspase-3-His₆ protein as the immunogen (Krajewska et al., 1997). The anti-peptide rabbit antibody recognizing cleaved subunits of caspase-3 (C3/MN-1) was generated using the peptide SGVDD-C after conjugation with KLH (Mashima et al., 1997). Affinity-purified His₆-tagged procaspase-9 recombinant protein was used as an immunogen to produce caspase-9 antiserum (AR-19) (Krajewski et al., 1999).

The additional polyclonal antisera for caspases were generated in rabbits using synthetic peptides or recombinant protein immunogens. Unless otherwise specified, peptides were synthesized with an N-terminal cysteine appended to permit conjugation to maleimide-activated carrier proteins KLH and OVA (Pierce, Inc.) as described previously (Krajewski et al., 1994b), and with a C-terminal amide (NH₂) rather than free carboxylic acid. New Zealand white female rabbits were immunized according to the previously described procedure (Krajewska et al., 2002b). Among the peptides employed as immunogens were: NH₂-(C)-PQPTFTLRKKLVPSPD-COOH (free acid) representing amino acids 51–69 of hu caspase-8 (AR-18), NH₂-CRPEIRKPEVLRPETPRPVD-amide representing amino acids 112–130 of hu caspase-9 (AR-20), NH₂-ALNPE-QAPTSLQDSIPAEAD-(C)-amide corresponding to residues 373–392 of hu caspase-10 (AR-21).

An additional anti-caspase-8 serum (AR-17), and antibodies specific for caspase-6 (AR-15), and -7 (AR-16) were generated using catalytic subunits of the relevant recombinant proteins fused with a C-terminal His₆-tag. Comparisons were made with a commercial anti-caspase-6 antibody (Upstate Biotechnology, Lake Placid, USA). Affinity-purified His₆-tagged recombinant human caspase-14 full-length protein was used as an immunogen to produce a polyclonal caspase-14 antiserum (AR-76). Since no dog-specific antibodies to apoptotic proteins were available, a series of immunoblotting experiments were performed to identify canine ortholog proteins specifically reacting with our antibodies, which were raised to human or mouse immunogens. In vitro translated or recombinant proteins, specimens from tissues with known endogenous expression of these proteins (mostly lysates from spleen and thymus), or tissue culture transfectants were used as positive controls and compared with the dog samples (not shown). The C9 knockout mice specimens were generously provided by Dr. Flavell, and had confirmed specificity of anti-caspase-9 antibodies. For all of the other proteins, there was no frozen or fixed material available from the relevant deficient mice. All antibodies (AR-#s) are available at BioCarta Inc, San Diego, CA (www.biocarta.com), Stratagene Inc. USA (www.stratagene.com) or Science Reagents, Inc., San Diego, CA (www.sciencereagents.com).

Immunoblotting and densitometry

Tissue lysates were prepared from the spleen, thymus, and duplicate hippocampal specimens of control-sham-

operated (three animals) or post-ischemic animals (six dogs), using modified RIPA lysis buffer (Upstate, Inc.). The lysates were normalized for total protein content (50 µg per lane) and subjected to SDS-PAGE/immunoblot analysis, using 1:1000–1:5000 (v/v) dilutions of antisera to Bcl-2 and caspase family members, and secondary HRP-conjugated goat anti-rabbit antibody (1:3000 v/v dilution) (Biorad). The detection was accomplished using an enhanced chemiluminescence (ECL) (Amersham-based) in conjunction with a multiple antigen detection (MAD) immunoblotting method that allows for multiple reproblings of blots, as described previously (Krajewska et al., 1994b, 1997).

ECL data on X-ray films were quantified by scanning densitometry using the Image-Pro Plus image analysis system (Media Cybernetics Co.). Relative band densities on Western blots were expressed as arbitrary densitometric units for each time points and presented as ratios relative to band densities observed in scans from loading control (F1-β-ATPase) on the same blot. The changes in expression of the proteins were confirmed in duplicate samples from the same animal and all investigations were performed in triplicates to assure the significance and specificity of the observations. The average of total counts was used to calculate the mean value per group at particular time points.

In vitro processing of recombinant caspase-14

Recombinant mouse caspase-14 (40 µg) was treated for 45 min at 37°C with mouse skin extract (20 µg), prepared according to Resing et al. (1989), or calpain I (2 units established from human erythrocytes; Calbiochem Inc.) in 250 µl of caspase buffer supplemented with 1 mM DTT and 1 mM CaCl₂. Detection of cleavage products was performed by SDS-PAGE immunoblotting with anti His-tag antibodies (Qiagen) or rabbit antibodies to caspase-14 (AR-76).

Immunohistochemistry

Dewaxed tissue sections were immunostained using a diaminobenzidine (DAB)-based detection method as described in detail, employing either an avidin–biotin complex reagent (Vector Laboratories) or the Envision-Plus-Horseradish Peroxidase (HRP) system (DAKO) using an automated immunostainer (Dako Universal Staining System) (Krajewski et al., 1994a, 1994c, 1997, 1999, 2002b).

The controls for the specificity of the immunostaining procedure were performed in parallel using preimmune serum or antiserum preabsorbed with 5–10 µg/ml of either synthetic peptide or recombinant protein immunogen.

The scoring of immunostaining for normal and ischemic foci in cerebral cortex and hippocampal sectors was based on the percentage of immunopositive cells (0–100) multiplied by staining intensity (0–3), yielding scores of 0–300. The immunostained slides were evaluated blindly by two independent investigators (MK and SK). The final scores were averaged. Utilizing ImagePro 4.1 morphometry soft-

ware (Media Cybernetics Co.), the densitometry, which is the stain intensity measurement that discriminates 256 levels of color saturation in all cellular compartments, was initially set on an arbitrary scale for intensities from 0 to 3 that can be differentiated by the human eye.

For double-labeling experiments, tissue sections were stained as above using a combination of rabbit polyclonal antisera and mouse monoclonal antibodies in conjunction with species-specific secondary antibodies. The antibodies used for these studies included monoclonal anti-cytochrome *c* (Pharmingen/BD Inc., La Jolla, CA, USA) and a polyclonal antibody against S100 protein, a pan-marker of glia. The staining for the monoclonal marker was accomplished using a ABC-HRP system (Vector Lab. Inc., Burlingame, CA, USA) and chromagen diaminobenzidine (DAB; Dako Inc., USA), which produces a brown color, followed by detection of the polyclonal antibody using alkaline phosphatase staining with Vector Red or BCIP/NBT development (Vector Lab. Inc), which yield red or blue colors, respectively. Slides were viewed by bright field or fluorescence microscopy.

TUNEL assays

The detection of nuclei with fragmented DNA by terminal deoxynucleotidyl transferase [TdT] end-labeling (“TUNEL assay”; ApopTag™, Oncor Inc.) was performed as a single- or two-color analysis (Krajewski et al., 1995), using the colorimetric substrates DAB and either VIP or SG (Vector Labs. Inc.) for TUNEL and Bcl-2 or caspase-family proteins, respectively.

Quantitative analysis of immunohistochemistry

All hippocampal cross-sections were studied immunohistomorphometrically by a computerized system. The sections were derived from three different animals at 0-, 30-min, and 2-h time points and four animals at 4-, 24-, and 48-h time points. The entire hippocampal CA1–CA2 and CA3 sectors from both hemispheres were scanned and digitalized at 20× magnification, using the Spot Advanced Imaging System (Diagnostic Inst., Sterling Heights, MI). The images imported into the Image-Pro plus 4.1 program (Media Cybernetics LP, Silver Spring, MD) were used to perform the morphometry. The method requires preliminary software procedures of spatial calibration (micron scale) and setting of color segmentation for quantitative color analysis.

The segmentation functions of the program were used to discriminate normal nuclei from the dark blue, condensed apoptotic nuclei in hematoxylin counterstaining, regardless of the specific marker immunoreactivity in the cytosol. Only hippocampal pyramidal neurons but no macroglia cells were counted. Total counts of pathological nuclei were used to calculate the mean value per group at particular time points. The average values from five measurements performed on representative coronal section in both hippocampi for each

case were interpolated at different time points of our observations. Means \pm SEM were calculated using unpaired *t* tests. The mean numbers of immunopositive or -negative neurons found in hippocampal sectors in both hemispheres from all animals at each time point were converted into percentages of total cell count obtained in CA1–CA2 or CA3 hippocampal sectors, respectively. Cell counts were analyzed using ANOVA with Bonferroni's post hoc analysis. Values given are means \pm SD per time group of animals. Differences were considered significant when $P \leq 0.05$.

Results

A recent survey of the dog genome sequence (6.22 million sequence reads; $1.5\times$ coverage) revealed that almost twice as much unique human sequence could be aligned with the $1.5\times$ collection of dog sequences than with the more complete $8\times$ collection of mouse sequences (O'Brien and Murphy, 2003). Therefore, the alignment of human peptide or recombinant protein sequences used for antibody production revealed 85–100% homology with dog relevant genes. These results suggest strong evolutionary conservation. The anti-caspase-7 antibody was the only antiserum that failed to react with its canine counterpart in immunoblotting experiments.

Immunoblot analysis of caspases and Bcl-2 family proteins in the post-ischemic brain

Figs. 1A–G show evidence that the various anti-caspase antisera are specific for their intended targets, using a panel of recombinant caspase-3, -6, -7, -8, -9, -10, and -14

proteins. Note that all of these antisera react uniquely with the appropriate caspase, with the exception of the anti-caspase-7 antiserum, which exhibits weak cross-reactivity with caspase-6. Loading of equivalent amounts of all caspase proteins was confirmed by various methods, such as reprobing the blot with anti-His₆ antibody when proteins were produced with His₆-tags (Fig. 1H) or in vitro translation in the presence of ³⁵S-L-methionine (not shown).

Figs. 2 and 3 reveal the representative intravital changes in the levels or proteolytic processing of these proteins in the canine brain following transient global ischemia. The hippocampus was chosen for these studies due to the documented role of apoptosis in ischemia–reperfusion injury in this ischemia-sensitive region of the brain (Krajewska et al., 1995; Sei et al., 1994). The changes in protein expression were confirmed on duplicate samples from the same animal. All investigations were performed in triplicates to assure the significance and specificity of the observations. The membranes were quantified by scanning densitometry and their mean density ratio is depicted in a graphic form in Figs. 2C and 3E.

With regards to Bcl-2 family proteins, two separate anti-peptide antisera, AR-04 and AR-05 that preferentially react with either Bcl-X_L or Bcl-X_S, respectively, (Krajewska et al., 1994c, 20002a) were employed. These two forms of the Bcl-X protein, which arise through alternative mRNA splicing mechanisms, have opposing effects on cell life and death, with Bcl-X_L functioning as a cell death blocker and Bcl-X_S as a promoter of apoptosis (Boise et al., 1993). The approximately 28-kDa Bcl-X_L protein was present in control sham-operated animals, whereas the approximately 19-kDa Bcl-X_S protein was not detected (Fig. 2A). Within 2 h of reperfusion, levels of Bcl-X_L declined 2.9-fold in

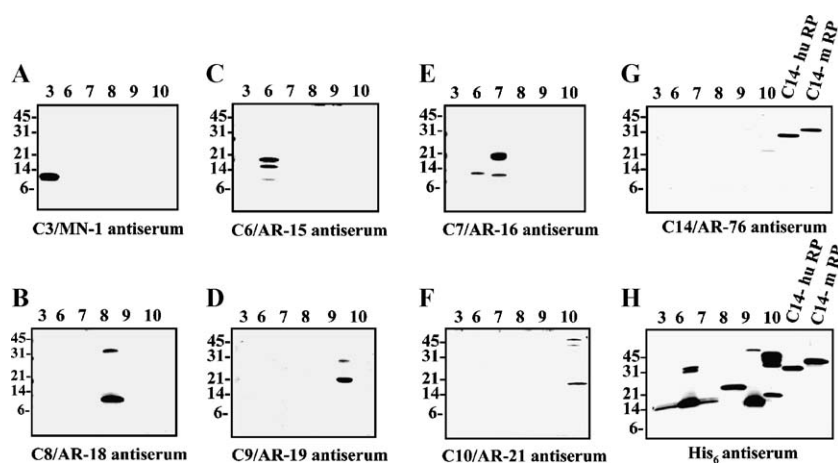


Fig. 1. Specificity of anti-caspase antibodies. Rabbit antisera, raised against either purified recombinant processed human caspase-6 (AR-15), caspase-7 (AR-16), purified recombinant mouse pro-caspase-14 (AR-76), or synthetic peptides corresponding to unique regions in caspase-3 (MN-1), caspase-8 (AR-18), caspase-9 (AR-20), and caspase-10 (AR-28) were tested for reactivity against recombinant purified caspases by immunoblotting. SDS-gels (12%) were loaded with 15 ng samples of recombinant proteins of active (processed) human caspases, except caspase-14 where the proforms of human and mouse proteins were used. Immunoblots were analyzed using antisera at 0.1–0.0125% (v/v) dilution and an enhanced chemiluminescence (ECL) detection system. All of these antisera react uniquely with the appropriate caspase, except anti-caspase-7 antiserum, which exhibits weak cross-reactivity with processed caspase-6. The same blot shown in (G) was probed with anti His-tag antibody, demonstrating loading of comparable amounts of all proteases (H).

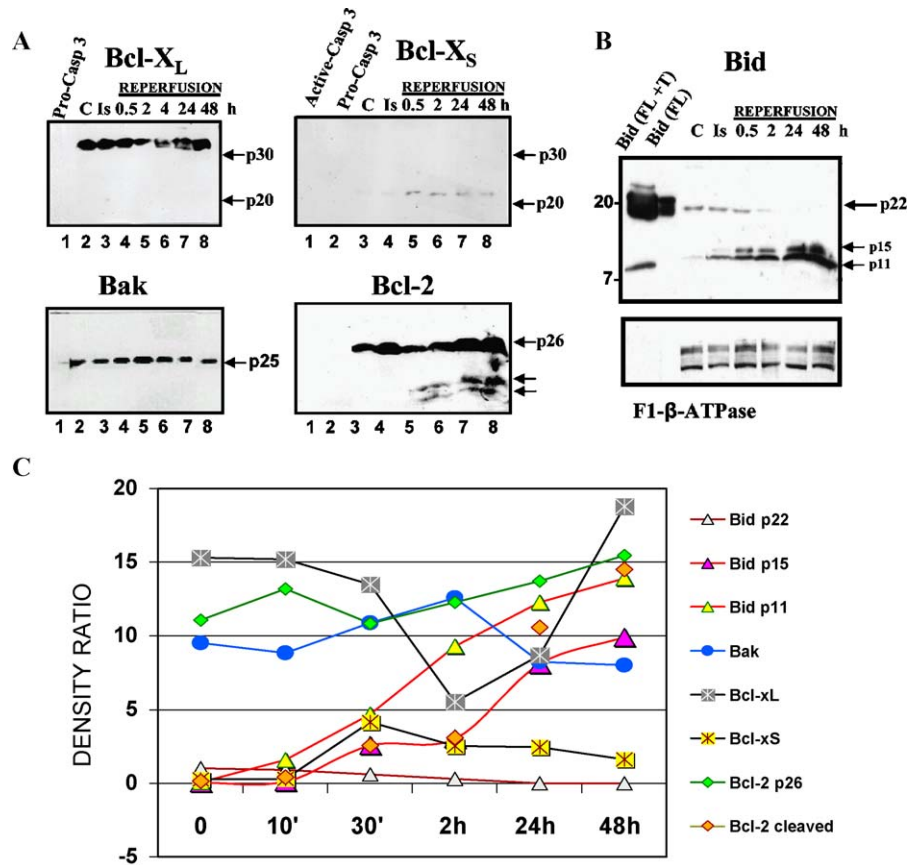


Fig. 2. Immunoblot analysis of Bcl-2 family proteins in hippocampus during ischemia and reperfusion. (A–B) Immunoblot analysis of canine hippocampal samples after sham operation (“C”), 10 min cardiac arrest alone (“S”), and for reperfusion periods from 0.5–48 h following cardiac arrest and resuscitation was performed, using multiple antigen detection method (Krajewski et al., 1996b). Antisera targeted against Bcl-X_L (AR-04), Bcl-X_S (AR-05), Bcl-2 (AR-01), Bak (AR-06), and Bid (AR-54) were employed. Samples (15 ng) of recombinant caspases or Bcl-2 family members, such as pro-caspase-3 and active caspase-3 (A) or full-length (FL) and truncated tBid (B) were included in some blots. (C) ECL data on X-ray films were quantified by scanning densitometry. The results for Bcl-2 family proteins are presented.

the hippocampus and remained lower for approximately 24 h, returning to pretreatment levels at 48 h (Figs. 2A, C). In contrast, Bcl-X_S protein became detectable within 30 min of reperfusion, reaching maximum levels at 30 min to 2 h of reperfusion, and slightly declining during 48 h post-ischemic insult (Figs. 2A, C). Thus, a transient decline of Bcl-X_L levels within 2 h of reperfusion was preceded by an 8-fold increase of Bcl-X_S levels. In contrast, levels of some other Bcl-2 family proteins remained relatively unchanged for approximately 2 days after transient cerebral ischemia. For example, Bak increase and Bcl-2 decrease remained within 1.5- and 1.4-fold of pretreatment levels, respectively, according to densitometry estimates, while Bcl-X_L levels dropped by nearly 3-fold (Figs. 2A, C).

Though Bcl-2 protein levels remained relatively unchanged during ischemia–reperfusion injury, novel approximately 23- and 19-kDa forms of Bcl-2 appeared beginning at approximately 2 h after resuscitation (Figs. 2A, C). Since it has previously been demonstrated that Bcl-2 can be cleaved by caspases (Cheng et al., 1997; Kirsch et al., 1999), these novel forms of Bcl-2 may represent caspase-cleaved molecules. The caspase-cleaved form of Bcl-2 has

been reported to enhance rather than inhibit apoptosis (Cheng et al., 1997).

The pro-apoptotic Bcl-2 family member Bid was expressed in the canine hippocampus before ischemic insult (Figs. 2B, C). Following 10 min of complete cerebral ischemia due to cardiac arrest and before reperfusion, a truncated approximately 11-kDa form of the Bid protein (tBid) was observed. Then, shortly after restoring reperfusion, levels of the full-length p22 Bid protein declined, and were replaced by an approximately 15-kDa truncated form of tBid. Since Bid is known to undergo cleavage by either caspases or lysosomal proteases, the generation of 11- to 14-kDa products depends on the cleavage site (Gross et al., 1999; Li et al., 1998; Stoka et al., 2001). We presume that the consumption of full-length Bid and generation of shorter forms of the protein results from protease cleavage, possibly involving both caspases and other proteases, for example, lysosomal enzymes and calpains (Chen et al., 2001).

Proteolytic processing of caspases was also demonstrated in the hippocampus, occurring after induction of reperfusion (at 30 min after cardiac arrest and reperfusion). Immunoblot

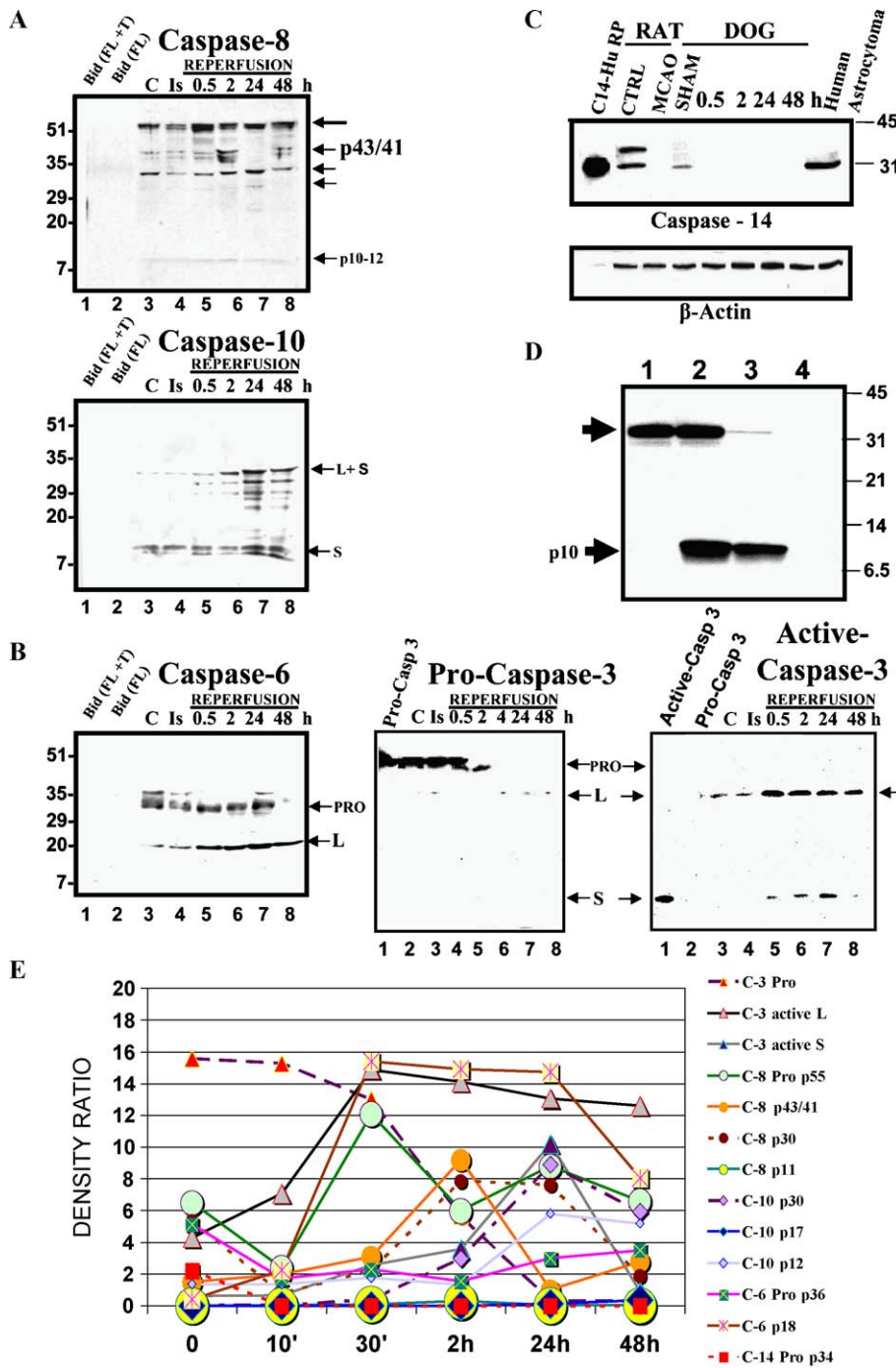


Fig. 3. Immunoblot analysis of caspases family proteins in hippocampus during ischemia and reperfusion. Antisera targeted against caspases (caspase-3/AR-14 and MN-1, caspase-6/AR-15, caspase-8/AR-18, caspase-10/AR-21, caspase-14/AR-76) were employed. The representative results are presented separately for the apical caspase-8 and -10 in A and executioner caspase-6, -3, and -14 in B–D. The positions of the endogenous proforms as well as processed large (L) or small (S) catalytic subunits of caspases are indicated by arrows. Panels C–D are dedicated to the experimentation on caspase-14, whose function, target substrates, and activation processing is at least known explored caspase so far. Tissue lysates from hippocampal gyri and cortical hemispheres of control sham-operated dogs and rats, respectively, show the approximately 32-kDa caspase-14 proform which disappears after ischemic injury (C). Middle cerebral artery occlusion (MCAO) in rats had been described previously (Gillardon et al., 1996a). A lysate from an astrocytic human tumor shows abundant amounts of pro-caspase-14, thereby providing further evidence of caspase-14 expression in brain. The same blot was reprobbed with anti-β-actin antibody (C) to confirm protein loading. (D) Mouse recombinant purified pro-caspase-14-His₆ protein (lanes 1–3) was incubated without (lane 1) or with calpain I (lane 2) or with mouse skin extract (lane 3). Lane 4 represents an equivalent amount of mouse skin extract incubated without recombinant pro-caspase-14. Proteins were analyzed by SDS-PAGE/immunoblotting using anti-His₆ antibody. The positions of the uncleaved pro-protein and cleaved p10 (small subunit) of caspase-14 are indicated by arrows (left). On E, the graphic summary of relevant densitometry results performed in similar way as for Bcl-2 protein family is demonstrated.

analysis of caspase-8 expression in the hippocampus of sham-operated dogs revealed a prominent approximately 55-kDa protein (Fig. 3A), consistent with full-length pro-caspase-8. Bands of p43/p41 and p10 were also evident, consistent with the partially processed fragments of this caspase which are known to be generated during apoptosis induced by recruitment of caspase-8 to TNF-family death receptors creating death inducing signaling complex (DISC) (Stegh et al., 2002). The DISC-associated p43/41 fragment of caspase-8 reached its peak levels at 2 h of reperfusion, and the p10 signal was noticeable within 30 min to 24 h after cardiac arrest and resuscitation (Figs. 3A, E). The two other bands indicated by arrows could correspond to additional anti-caspase-8 reactive proteins, possibly reflecting isoforms, which are known to arise by alternative mRNA splicing in humans (Scaffidi et al., 1997) (Figs. 3A, E).

Immediate proteolytic processing of pro-caspase-10 was also observed in the hippocampus after transient global cerebral ischemia. Our anti-caspase-10 antibody failed to react with the unprocessed pro-caspase-10 zymogen, but it detected the p12 small catalytic subunit (Fig. 3A). Levels of the small subunit of processed pro-caspase-10 increased approximately 4.3-fold after ischemia–reperfusion injury, becoming maximal at 1–2 days post-ischemia (Fig. 3E). Intermediate proteolytic processed forms of pro-caspase-10 were also detected beginning at approximately 2 h of reperfusion. The most prominent of these probably represents the caspase-10 zymogen with its N-terminal pro-domain removed, based on its estimated molecular mass in SDS-PAGE (Cohen, 1997).

Caspase-6 was analyzed using two different antibodies which either bind to unprocessed or processed proteases. Unprocessed pro-caspase-6 was detected in the hippocampus of sham-operated dogs by a commercially available antibody (Fig. 3B). Shortly following 10 min of cardiac arrest, levels of processed caspase-6 increased, as shown also by our antibody that reacts preferentially with the processed protein. The amount of processed caspase-6 rose by approximately 7-fold at 2–24 h of reperfusion, persisting throughout 48 h of observation (Figs. 3B, E). In contrast, an approximately 10-fold decline in the amount of unprocessed pro-caspase-6 was observed, starting at 2 days post-ischemia (Figs. 3B, E).

Caspase-3 is synthesized as a 32-kDa proform (zymogen) that is cleaved during activation to yield a large catalytic subunit of 20 or 18 kDa, depending on the apoptotic signal (Erhardt and Cooper, 1996), and a small catalytic subunit of 12 kDa (Nicholson et al., 1995). The analysis of caspase-3 was conducted using two different antisera, one which reacts with uncleaved pro-caspase-3 (approximately 32 kDa) as well as the large subunit of processed caspase-3 (Fig. 3B; antiserum AR-14), and another that reacts only with cleaved caspase-3 subunits (large and small) but not unprocessed pro-caspase-3 (Figs. 1A, 3B; C3/MN-1). Levels of unprocessed pro-caspase-3 declined 2.7-fold within 2 h of ischemia, with little or no detectable uncleaved pro-caspase-3 remaining after 4–48 h of reperfusion (Figs. 3B, E; AR-14). In contrast, levels of the cleaved large and small catalytic subunits of caspase-3 increased after ischemia, becoming apparent at 30 min and persisting throughout 48 h of reperfusion (Figs. 3B, E).

An anti-caspase-14 serum was produced in rabbits and used to examine expression of this protease in the brain. The mono-specificity of the antibody was confirmed by SDS-PAGE/immunoblot analysis (Figs. 1G, 3C). Two principal products were observed: (a) an approximately 30- to 32-kDa band consistent with unprocessed pro-caspase-14; and (b) an approximately 20-kDa band indicative of the processed large subunit of this protease. As expected from other reports (Hu et al., 1998; Van de Craen et al., 1998), abundant amounts of caspase-14 protein were detected in detergent lysates prepared from human epidermis, where additional fragments p14–16 and p10 were observed. Caspase-14 protein was also present at lower levels in the brain, and testis of humans and mice (not shown).

Having obtained evidence that caspase-14 is expressed in normal brain, we applied our anti-caspase-14 antibody for analysis of this protease in cerebral ischemia models. The 32-kDa proform of caspase-14 was detected in canine hippocampal specimens derived from sham-operated animals (Fig. 3C). In contrast, this protein was rapidly depleted from hippocampal tissue within 30 min of reperfusion. Similar results were obtained in a rat model of focal

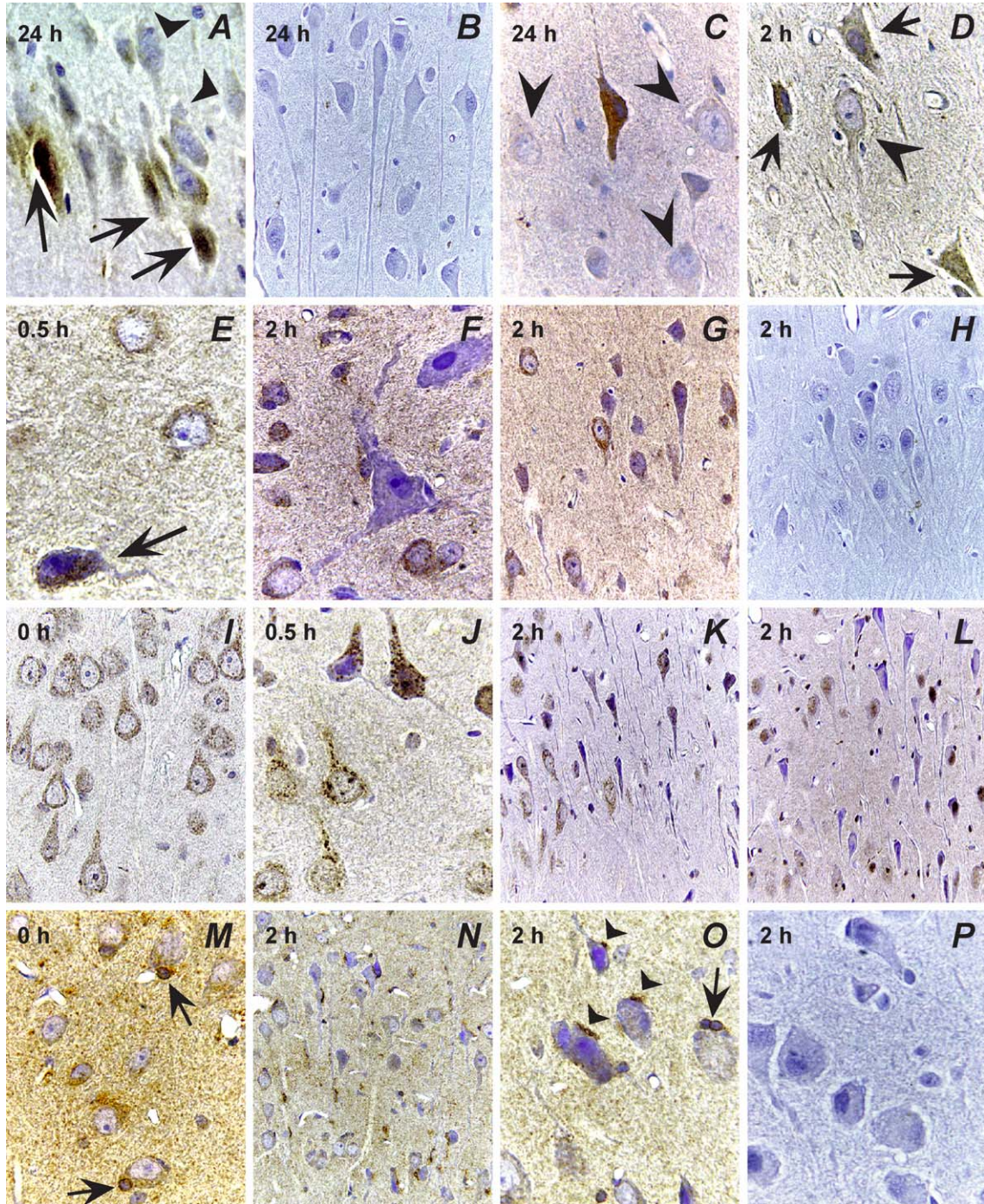
Fig. 4. Immunohistochemical analysis of Bcl-2-family proteins and apical caspases during global ischemia. Representative examples of immunohistochemical data are presented (150–1200× magnification). Ischemic neurons in CA1 hippocampal sectors displayed increased staining for Bcl-X_s compared to immunonegative normal neuronal cells (panel A; arrows). Panel B shows negative immunostaining using peptide-preabsorbed antiserum. (C) Elevated levels of Bax were observed in ischemic cortical neurons compared to morphologically unchanged neurons (arrowheads). (D) Bak expression in normal neurons was barely detectable (arrowheads). Increased Bak immunostaining was observed in affected CA1 hippocampal neurons (arrow). (E) Unlike normal neurons, degenerating cortical pyramidal neurons showed intense Bid staining (E; arrow) at 30 min reperfusion. At 2 h reperfusion, many neurons displayed loss of BID immunoreactivity in cortical layer III in large Betz pyramidal neurons (F) and CA1 hippocampal region in pyramidal neurons (G), respectively. (H) A sequential section from the hippocampus was stained using anti-BID antiserum, which had been preabsorbed with specific peptide. The dynamic of caspase-8 immunoreactivity is demonstrated in the cortex of sham-operated animals (I) and after reperfusion, in the CA1 sector of hippocampus (J–L). Caspase-8 immunostaining was performed using AR-17 (I–K) and AR-18 (L), respectively. (M–P) Low to moderate neuronal (M) and high oligodendroglial (M; arrows) immunoreactivity for caspase-10 in brains of sham-operated animals declined after reperfusion, as shown for CA1 hippocampal sector (N), and in cortex (O). In contrast to oligodendroglia in close proximity to undamaged neurons (O; arrow), dying satellite oligodendroglial cells in contact with degenerating neurons contained perisomatic intense caspase-10 immunostaining (N, O; arrowheads). (P) Control staining is shown, using AR-21 preabsorbed with caspase-10 peptide.

ischemia, where pro-caspase-14 was immunodetectable in mock-treated animals but not in ischemic brain tissue from animals subjected to middle cerebral artery occlusion (MCAO; Fig. 3C). Reprobing the same blot with anti- β -Actin antibody confirmed loading of approximately equivalent amounts of total protein. An *in vitro* experiment revealed that calpain I and proteases present in extracts of mouse epidermis cleaved recombinant mouse caspase-14 (Fig. 3D) to generate fragments of approximately the same size as those observed in specimens derived from the human brain and epidermis. It remains to be determined if calpains

are responsible for caspase-14 processing *in vivo* in the brain during ischemia–reperfusion injury.

Immunohistochemical analysis of Bcl-2-family proteins in ischemia-sensitive regions of the brain

Immunostaining for Bcl-2 family proteins revealed the most profound changes in immunoreactivity in the ischemia-sensitive regions of the brain, particularly the (a) hippocampal sectors CA1, CA2, and CA4; (b) basal ganglia, including striatum and intrathalamic nuclei, (c) cerebral



cortex layers III–V (particularly in the depth of gyri); and (d) cerebellum, especially the Purkinje cell layer. Representative data are presented in Fig. 4. The ischemia-resistant regions of the brain served as internal controls when evaluating changes in immunointensity.

Within 30 min to 2 h after resuscitation following 10 min of global ischemia, various neuronal subpopulations exhibited reductions in the immunoreactivity for the Bcl-2 and Bcl-X_L proteins. At 2 h reperfusion, the expression of both proteins in neurons with morphological features of acute ischemic degeneration uniformly declined. In contrast, immunoreactivity for Bcl-X_S (AR-05) appeared within 30 min to 2 h after cardiac arrest and resuscitation in ischemic-damaged neurons (Fig. 4A). Consistent with prior reports in rodent models (Antonawich et al., 1998; Gillardon et al., 1996b; Isenmann et al., 1998; Krajewski et al., 1995), immunostaining for the pro-apoptotic protein Bax also increased in affected neurons after ischemia/reperfusion (Fig. 4C). Again, Bak protein immunoreactivity was observed, particularly in the pyramidal neurons of the cortex (cortical layers III–V), at regions of borderline vascularization (Zulch and Gessaga, 1972), and in hippocampal sectors CA1, CA2, and CA4 (Fig. 4D). When cells exhibited early signs of degeneration, both Bax and Bak proteins resided within the neuronal cell bodies in a granular (mitochondria-like) pattern. In shrunken cells with advanced deterioration, the immunostaining sometimes overlaid the nucleus as well.

In the normal canine brain, Bid was constitutively expressed in many neuronal subpopulations throughout the central nervous system. Moderate intensity cytosolic immunostaining was seen, for example, in the pyramidal neurons of the hippocampus (sectors CA1–4), cortex, basal ganglia, and in the mitral cells of the olfactory bulb. In contrast, the small granular neurons of the olfactory bulb, hippocampal dentate gyrus, and cerebellum exhibited

only low-intensity Bid staining. Neuroglia within control brains contained moderate (satellite oligodendroglia and in the white matter) or low (ependyma, astroglia) Bid levels. Moderate Bid immunoreactivity was present in the neuropil and axons (both in the cortex and in the white matter), while the axons of cranial peripheral nerves were strongly positive for Bid. As early as 30 min after initiating reperfusion, striking depletion of Bid immunoreactivity was observed in neurons suffering acute post-ischemic changes within the ischemia-prone regions of the brain (CA1 hippocampal sector, cortical layers III–VI, basal ganglia/thalamic nuclei, Purkinje cells/cerebellum, reticular formation/brain stem). Interestingly, in some types of neurons, particularly the Purkinje cells of the cerebellum and the large motoneurons within cranial nerve nuclei, the intracellular location of Bid immunostaining was suggestive of translocation of the Bid protein to cell organelles (presumably mitochondria) within cells displaying early morphological signs of post-ischemic degeneration (Fig. 4E; arrow). By 24 h after ischemia–reperfusion injury, Bid immunoreactivity had completely disappeared from the cell bodies of affected neurons (Figs. 4F, G).

Initiator caspases

The patterns of immunostaining were examined for the upstream initiator proteases, caspase-8, and -10. Using two different anti-caspase-8 antibodies, cytosolic caspase-8 immunostaining was found in both neurons and glia throughout the CNS of sham-operated dogs (Fig. 4I). Moderate-intensity caspase-8 immunostaining was observed in most neuronal cell bodies and the surrounding neuropil (dendrites mostly), while axons generally contained weaker caspase-8 immunostaining. In contrast to most other neurons, however, Purkinje cells of the cerebellum were immunonegative. Among the glial cells,

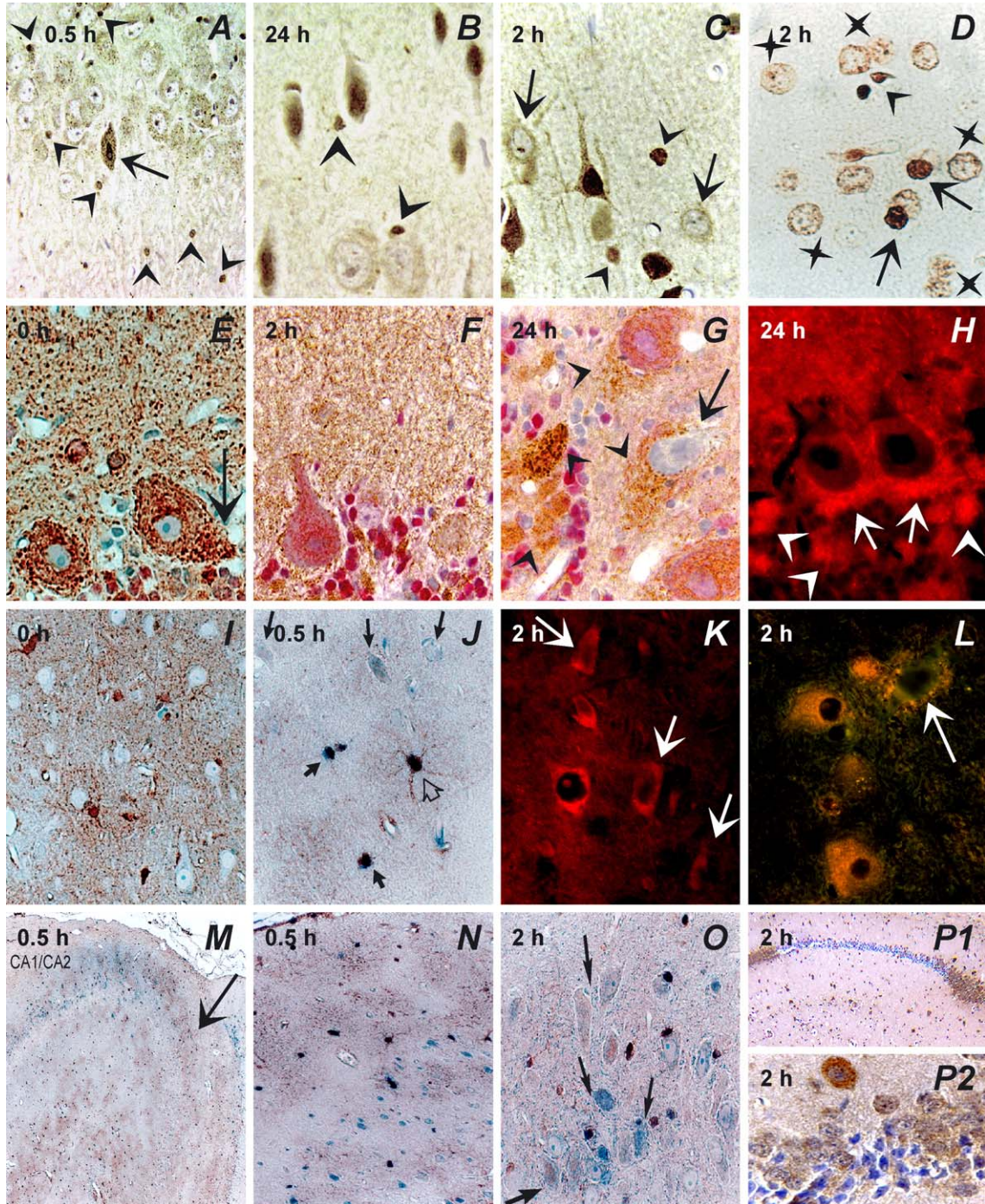
Fig. 5. Immunohistochemical and immunofluorescence analysis of executioner caspases, cytochrome *c*, and neuroglia marker S-100 in post-ischemic brain. In A, in addition to cytoplasmic staining, occasional neurons in hippocampus CA1 sector demonstrated immunoreactivity for processed caspase-3 both in cytoplasm and nucleus (arrow), while many neuroglia cells showed strong nuclear staining at 0.5 and at 24 h after reperfusion (B) before neurons (arrowheads). (C) In cortical layer III, degenerating neurons contained increased cytoplasmic caspase-6 staining alone or in combination with strong nuclear immunoreactivity. Surrounding oligo- and astroglia exhibit similar strong nuclear immunostaining for caspase-6 (arrowheads). Unchanged neurons are indicated by arrows. (D) A sequential tissue section from the same area as panel C was analyzed for DNA fragmentation by the TUNEL assay. Note the strong TUNEL reaction in the nuclei of astroglia (arrows) and oligodendroglia (arrowhead), while most neurons remain TUNEL-negative (asterisk). (E–G) Cerebellum was analyzed using a two-color method for simultaneous detection of cytochrome *c* (brown) and caspase-6 (pink-red). In morphologically normal Purkinje cells from a sham-operated animal (E), cytochrome *c* displays a coarse-granular pattern in cell bodies, dendrites, and in the basket cell synapses on the Purkinje cell bodies (arrow). Negligible staining for caspase-6 is seen in these morphologically normal cells (E). At 2 h post-reperfusion, caspase-6 staining was noticed also in the nuclei of degenerating Purkinje cells (F). After 24 h of reperfusion, Purkinje cells with advanced degeneration showed significantly reduced levels of both markers (G). Strong cytochrome *c* immunostaining remains present only in the basket cell synaptic contacts upon Purkinje cell bodies and glomeruli (arrowheads) (G), as shown also by dark field microscopy (H). (I) In brains of sham-operated animals, macroglia did not contain caspase-6 immunoreactivity (here in the parietal cortex). (J) In ischemic foci, downregulation in immunostaining for neuroglial marker S-100 (brown) and simultaneous increases of immunostaining for active caspase-6 (blue) were observed in astroglial cells (thick arrows) and in neighboring pyramidal neurons with apoptotic morphology (thin arrows). An adjacent normal astroglial cell is indicated by an open arrow. (K, L) Using dark-field microscopy and single-color immunostaining with a fluorescent (red) substrate, decreasing diffuse pattern of cytochrome *c* was found in ischemic neurons of cortex (K) and thalamus (L) at 2 h of reperfusion. (M, N) The double-labeling technique used for panels (I) and (J) was applied here. CA1–CA2 sectors of hippocampus show evidence of depletion of S-100 macroglia at early times (0.5 h) of reperfusion, accompanied by increased caspase-6 immunostaining in their nuclei (on N at high magnification). (O) Later, dying neurons in the cortex often contained strong nuclear caspase-6 immunostaining (arrows) along with low levels of cytosolic staining. (P1–P2) The panels demonstrate at low and high magnification the representative example of caspase-14 immunostainings in the CA2/C3 hippocampal sectors, 2 h after global ischemia.

the satellite oligodendroglia of the cortex and fibrillary astroglia in the white matter expressed the strongest caspase-8 immunoreactivity.

The caspase-8 immunostaining pattern changed rapidly in selected cell populations after cardiac arrest. The cytosolic staining of glial cells, for example, was replaced by strong nuclear staining, particularly in oligodendroglia. In neurons featuring signs of early ischemic injury, a coarse-grain accumulation of caspase-8 immunoreactivity was seen in the cytosol, suggesting association with organelles or filaments (Fig. 4J). In the cerebral cortex, basal ganglia, and

hippocampus, a gradual loss of cytosolic caspase-8 immunoreactivity occurred, accompanied by a gain in nuclear staining which generally reached maximum intensity at 2 h of reperfusion (Figs. 4K, L). By 24 h of reperfusion, most of the caspase-8 immunoreactivity disappeared from neurons exhibiting morphological evidence of degeneration. Two different anti-caspase-8 antibodies generated against either a synthetic peptide or recombinant protein produced the same results.

Caspase-10 showed a similar expression pattern to caspase-8 throughout the CNS in sham-operated dogs (Fig.



4M). The immunoreactivity declined in the neurons of the ischemia-sensitive regions of the brain within 30 min of reperfusion, with minimal expression remaining at 24 h (Fig. 4O). However, degenerating satellite oligodendroglia in the vicinity of ischemic neuronal cell bodies within the hippocampal sectors CA1–CA2, cortical layers III–VI, and particularly around large Betz neurons in the motocortex contained augmented caspase-10 immunolabeling in their remnants (Figs. 4N, O; arrowheads).

Caspase-9 immunoreactivity in this canine model has been previously described (Krajewski et al., 1999), and thus the results are not presented here.

Effector caspases

The expression of the downstream effector proteases, caspase-3, -6, and -7, was examined. Two antibodies were used to characterize the involvement of caspase-3 in the post-ischemic brain. The AR-14 antiserum was generated against recombinant unprocessed human caspase-3 and primarily displays affinity to the unprocessed proform of caspase-3 in immunostaining experiments (Krajewska et al., 1997). The anti-peptide (C3/MN-1) antibody reacts preferentially with active processed caspase-3 and was raised against a sequence corresponding to junction between the large (C-termini end; 175–180 amino acids) and small catalytic subunits. With the antibody detecting unprocessed pro-caspase-3, low levels of caspase-3 immunoreactivity were detected in most types of glia and neurons. A transient signal increase in cytosol of ischemia-sensitive neurons within 30 min after cardiac arrest and resuscitation was followed after 2 h by reduction of caspase-3 levels in neurons displaying morphologic features of ischemic degeneration. At 24–48 h of reperfusion, a complete loss of pro-caspase-3 cytosolic expression was observed in extensively shrunken neurons, with a few neuronal cells showing faint nuclear staining.

With the antiserum that preferentially reacts with processed (active) caspase-3, brain sections from sham-operated dogs were largely immunonegative. However, after cardiac arrest and resuscitation, a marked increase in immunostaining of both cytosolic and nuclear compartments of ischemia-damaged neurons was evident as early as 2 h of reperfusion (Fig. 5A; arrow). At later stages (24–48 h), active caspase-3 immunostaining was largely confined to the nucleus, with little residual cytosolic staining seen (Fig. 5B). Additionally, occasional astrocytes, numerous oligodendrocytes, and satellite perineuronal glia contained activated caspase-3, in both the cytoplasm and the nucleus (Figs. 5A, B; arrowheads).

Using the anti-caspase-6 antiserum that reacts preferentially with the processed protease, low caspase-6 immunoreactivity was observed in the cytosol of cerebral neurons in the brains of sham-treated animals. Contrary to active caspase-3, immediately after initiating reperfusion, caspase-6 immunoreactivity increased predominantly in the nuclei of glial cells

(Fig. 5C; arrowheads), and subsequently in the cytosol and nuclei of neurons in the cortex (Figs. 5C, J), Purkinje cells in the cerebellum (Figs. 5F–G) and the CA1 sector of hippocampus at 2 h, and in the granular neurons of the dentate gyrus at 24 h. However, primarily mostly nuclear elevated caspase-6 expression in the degenerating pyramidal neurons of the CA1 sector declined at 24 h. This evidence suggests that the increase in caspase-6 immunoreactivity is transient following ischemia–reperfusion injury. Neighboring neurons that retained normal morphological appearance contained mostly low intensity cytosolic caspase-6 immunostaining and were TUNEL-negative (Fig. 5C; arrows and 5D).

Caspase-14 immunoreactivity was detected in neuronal and glial cells in the normal canine brain. After cardiac arrest, caspase-14 immunoreactivity was rapidly lost in neurons in the ischemia-prone regions of the brain (Fig. 5, P1–P2).

*Changes in location of cytochrome *c* in ischemia-damaged brain*

Since cytochrome *c* is known to be released from mitochondria into the cytosol and then induces activation of certain caspases (reviewed in Green and Reed, 1998), we evaluated the in situ location of this protein by immunohistochemical analysis of brain sections taken from sham-operated (control) and post-ischemic brain. In addition, two-color immunocytochemical analysis of caspase-6 and cytochrome *c* distribution in the normal and ischemic brain was performed. In the cerebellum, Purkinje cells in sham-operated animals exhibited an intense, punctate cytochrome *c* immunostaining pattern (Fig. 5E; brown from DAB) indicative of mitochondrial localization (Green and Reed, 1998). Immunodetectable caspase-6 was negligible in these cells. In contrast, as early as 0.5–2 h of reperfusion, cytochrome *c* staining was distributed diffusely through the cytoplasm, indicating that this protein had been released from mitochondria (Fig. 5F). The markedly elevated cytosolic immunoreactivity of caspase-6 (red from Vector Red) was detected by our antibody that preferentially reacts with the processed form of this protease (Fig. 5F).

At 24 h reperfusion, Purkinje cells with advanced degeneration (“ghost cells”) were immunonegative for caspase-6 and cytochrome *c*, suggesting degradation of these proteins (Fig. 5G; arrow). In contrast, the cytochrome *c* pattern in mitochondria-rich basket cell synapses was unchanged during ischemia–reperfusion (Fig. 5G; arrowheads), demonstrating that release of cytochrome *c* is highly localized to ischemia-sensitive Purkinje cells. Also, at 2–24 h reperfusion, many of the granular cell neurons contained nuclear caspase-6 immunostaining (red), implying that these cells may activate their apoptotic program in a similar fashion to the ischemia-vulnerable Purkinje cells (Figs. 5F, G). The small size of these granular cell neurons precluded an analysis of cytochrome *c* distribution.

Astro- and oligodendroglial apoptosis following ischemia–reperfusion injury

In our study, strong immunostaining for Bid and the initiator proteases, caspase-8 and -10, was found in astro-dendroglia and particularly in oligodendroglia. During is-

chemia and reperfusion, the first changes in caspases immunostaining patterns were noticed in macroglia, which demonstrated widespread strong nuclear staining for caspase-8, -10 and for active caspase-6. These findings were associated with depletion of Bid immunoreactivity and increased TUNEL positivity. Interestingly, TUNEL posi-

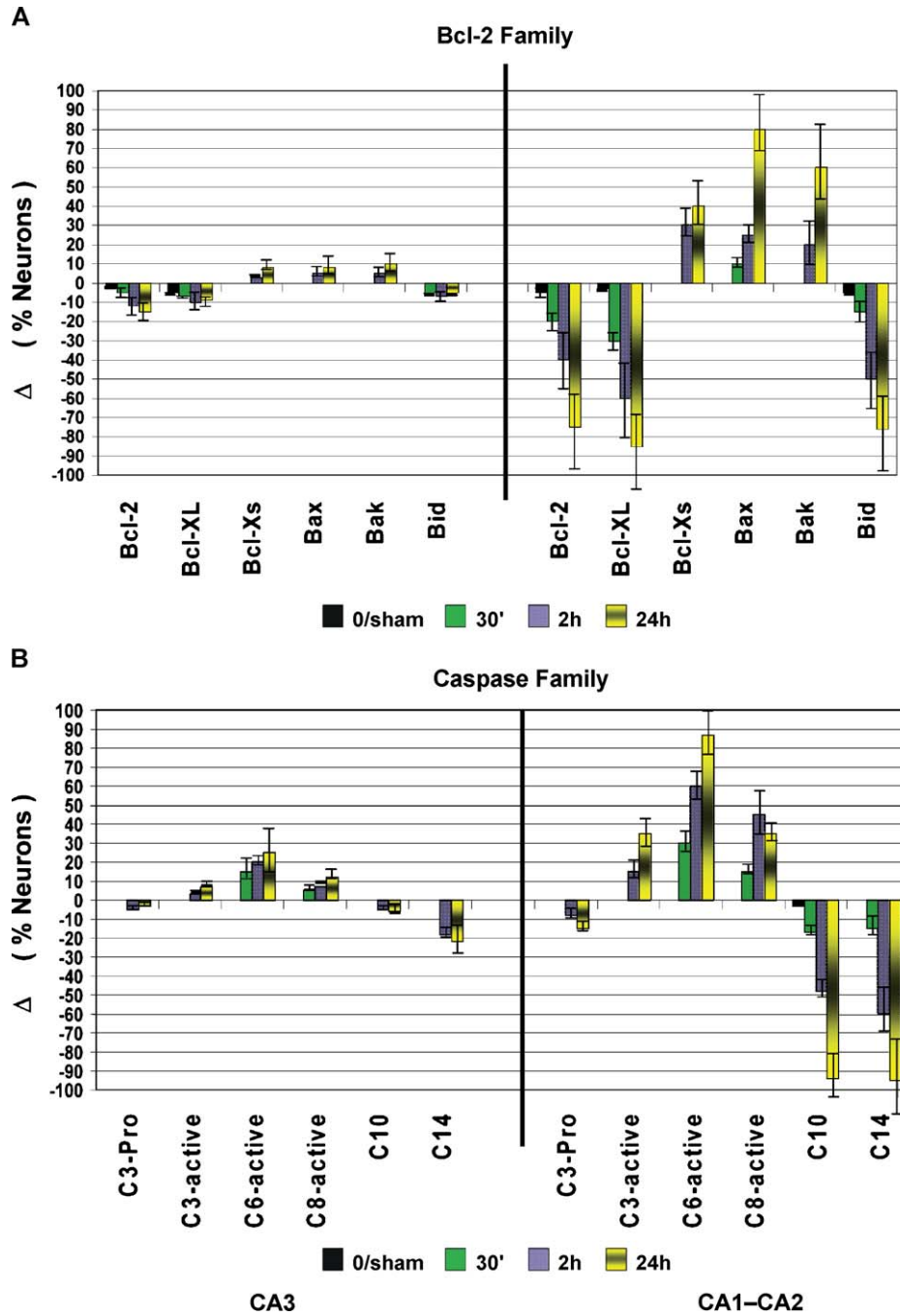


Fig. 6. Quantitative analysis of immunohistochemistry. For quantitative analysis of immunohistochemistry, the entire hippocampal CA1–CA2 and CA3 sectors in both hemispheres were scanned and digitalized at 20× magnification, using an imaging system with morphometry software. The sections were derived from three different animals for sham-operated controls and 30-min, 2-h reperfusion time points, and five animals for the 24-h reperfusion period. The neuronal cells presenting elevated levels of proteins were plotted as positive, while those with reduced levels were plotted as negative on the y-axis. The evaluation was performed by two independent observers. Cell counts were analyzed with ANOVA and Bonferroni's post hoc analysis. Data represent mean ± SD for the Bcl-2 family proteins (A) and caspases (B), showing percentage of neurons exhibiting a change in staining intensity.

vity of glia typically preceded morphological changes of nuclei (Fig. 5D).

Double labeling of macroglia for caspase-6 (marked blue with alkaline phosphatase) and a glial cell antigen S-100 (marked brown with DAB) revealed negligible signals for caspase-6 in glial cell bodies and their processes in the normal CNS (Fig. 5I). After ischemia/reperfusion, increased immunopositivity for active caspase-6 and a sharp reduction of S-100 staining were seen in degenerating glial cells (Figs. 5J, M–O).

Quantitative analysis of immunohistochemistry

A quantitative analysis of immunohistochemical staining results was performed in arbitrary fashion for pyramidal neurons of the entire CA1/CA2 (sensitive) and CA3 (resistant) sectors in both hippocampi (Fig. 6). The percentage of neurons demonstrating a change in immunointensity relative to control neurons (down- or upregulation) was determined for all animals at each time point (0/sham, 30 min, 2 and 24 h) using an imaging system with morphometry software. The mean percentage of neurons with changes in immunostaining was plotted separately for Bcl-2-family proteins (Fig. 6A) and caspases (Fig. 6B) at four time points (0/sham, 30 min, 2 h, and 24 h). Note that in the CA3 ischemia-resistant sector during the entire experiment, the number of neurons showing increased or decreased immunoreactivity different from normal expression pattern did not exceed $\pm 20\%$, compared to 85% in CA1. Statistically significant post-ischemia increases in CA1 sector neurons were documented for Bcl-X_S, Bax, Bak, caspase-6, and -8, while post-ischemia reductions were noted for Bcl-2, Bcl-X_L, Bid, caspase-10, and -14 ($P < 0.005$).

Discussion

Mechanisms of neuronal cell death following ischemia injury have been studied extensively in rodent models. However, during evaluation of novel agents for neuroprotective activity in stroke, it is well established that data from rodent models are not fully predictive of experiences in human clinical trials (Forsting et al., 1994). Similar issues were recently addressed by an NIH panel, the Stroke Progress Review Group (SPRG, Report of the Stroke Progress Review Group. NINDS 2002). One of the recommendations of the review panel was that animal modeling of cerebral ischemia must be carried out in other species besides rats. In particular, they stressed the need for increased usage of large animal models of cerebral ischemia.

Thus, a need exists to confirm and extend data about molecular mechanisms of ischemia-induced neuronal cell loss to alternative animal models. To this end, we reported the first data concerning core regulators of apoptosis in a large animal model of global cerebral ischemia.

We elected to employ a model of transient global ischemia involving cardiac arrest followed by resuscitation for our analysis of apoptosis proteins because of the evidence that apoptotic cell death occurs in this setting. In this regard, caspases are a family of cysteine proteases that play a central role in the initiation and execution of apoptosis (Thornberry and Lazebnik, 1998). Our analysis reported here for caspase-8 and -10, in conjunction with our previous report on caspase-9 (Krajewski et al., 1999), provides evidence that both the mitochondrial and death receptor-mediated pathways for caspase activation are triggered in the canine brain following transient global ischemia. The immunoblot analysis revealed an early processing of caspase-8 and -10 (within 2 h of reperfusion), with a gradual increase of small subunit of processed caspase-10, reaching peak levels at 1–2 days post-ischemia. Although caspase-8 and -10 activation was generally described in spatiotemporal relationships with delayed cell death (Jin et al., 2001; Velier et al., 1999), a few reports showed early activation of caspase-8 in a model of focal ischemia (Benchoua et al., 2001) or transient spinal cord ischemia (Matsushita et al., 2000). The differential expression of the active forms of caspase-8 and -3 in cortical neurons after permanent focal stroke in rats (Velier et al., 1999) contributes to the hypothesis that specific apoptosis pathways may be activated among the populations of brain neurons.

Among effector caspase-3 and -6, our observations suggest immediate activation, that is, within 30 min reperfusion, and redistribution of caspase-6 before active caspase-3, which occurred latter at 2–24 h of reperfusion period. Although activation of caspase-3 following injury to brain and spinal cord is well established (Gillardard et al., 1997; Namura et al., 1998; Sasaki et al., 2000; Springer et al., 1999), little is known about caspase-6 processing after cerebral ischemia. In rodent models, similar time points for caspase-3 activation have been reported, with an early peak at 6–24 h (Cho et al., 2003), and a delayed peak 2–3 days after ischemia. Active caspase-3 in dendrites and axons was found to be responsible for a transynaptic execution of neuronal death in vulnerable sectors of hippocampus (Rami et al., 2003). The temporal sequence of caspases processing seen here raises the possibility that caspase-6 activation occurs upstream of caspase-3 or via an alternative pathway independent from caspase-3. In addition, we obtained evidence here that cytochrome *c* is released from mitochondria in neurons after ischemia–reperfusion injury in the dog model, implying direct activation of the caspase-9 pathway for apoptosis.

Regardless, broad-spectrum caspase inhibitors have been shown to abrogate ischemic injury after global (Chen et al., 1998; Himi et al., 1998; Vogel et al., 2003) and focal ischemia (Endres et al., 1998; Fink et al., 1998; Ma et al., 1998; Onteniente et al., 2003). Ischemic brain injury is also reduced in caspase-3 knockout mice (Le et al., 2002), strongly suggesting an important role for this and other

caspsases in neural cell death caused by cerebral ischemia and reperfusion.

Development of apoptotic morphology is still considered the gold standard for apoptosis identification (Darzynkiewicz et al., 2001). DNA fragmentation is usually detected by in situ techniques such as the TUNEL assay. In our study, changes in intracellular distribution of caspsases were generally seen before evidence of DNA fragmentation. For example, immunostaining for caspsase-8, -6, -3 and -9 appeared to converge on the nuclei of ischemia-damaged neurons, many of which were TUNEL-negative. This finding suggests that caspsase activation precedes DNA fragmentation in ischemia-damaged neurons in this animal model, consistent with the sequence of events demonstrated for apoptosis induction in vitro in neurons and other types of cells. Similar observations have been made by others, at least for caspsase-3 and -8, using rodent models of brain ischemia or brain trauma (Chen et al., 1998; Namura et al., 1998; Velier et al., 1999). While caspsase activation and DNA fragmentation are normally associated with apoptosis, studies indicate that both events can occur during, and contribute to cell injury that eventually culminates in necrosis (Atlante et al., 2003; Jaeschke and Lemasters, 2003; Neumar et al., 2003; Niquet et al., 2003; Wang et al., 2003). The potential involvement of caspsases and other “apoptotic” proteins in necrotic cell death is particularly relevant to our cardiac arrest model of global cerebral ischemia. We observed a mixture of both apoptotic and necrotic neuronal morphologies using this model (Rosenthal et al., 2003).

Caspase-14 is the most recently discovered member of the caspsase family in mammals (Ahmad et al., 1998; Hu et al., 1998; Van de Craen et al., 1998). The role of caspsase-14 in apoptosis has not yet been clarified. Unlike other caspsases, caspsase-14 is cleaved at Ile152 and Lys153, producing fragments with homology to the p20 and p10 subunits, but no substrates of this caspsase have been described (Chien et al., 2002). Highly expressed in embryonic tissues, expression of caspsase-14 mRNA in several adult organs was reported by Ahmad et al. (1998) but was claimed to be limited predominantly to epidermis by others (Hu et al., 1998; Van de Craen et al., 1998). In brain tissue, von Mering et al. (2001) showed elevation of caspsase-14 mRNA after inducing bacterial meningitis in mice. In the present study, abundant amounts of caspsase-14 protein were detected by immunoblotting, predominantly in epidermis, but also in brain and some other tissues. We also discovered that pro-caspase-14 is rapidly depleted from the canine hippocampus after induction of ischemia. These results are consistent with, but do not prove, activation of caspsase-14 during ischemia–reperfusion injury in the brain. Interestingly, we show in vitro that recombinant mouse caspsase-14 was cleaved by calpain I as well as by proteases from mouse epidermal extracts. However, selective substrates of caspsase-14 must be identified before caspsase-14 protease activity can be measured directly. We were unable to obtain processing of human caspsase-14 by calpain I in vitro

experiments. The latter result is in agreement with another report (Chien et al., 2002).

Although caspsases represent the principal effectors of apoptosis, Bcl-2-family proteins function by governing the mitochondria-dependent cell death pathway and often dictate whether caspsases become activated. We obtained evidence of several changes in either the expression or proteolytic processing of Bcl-2-family proteins following ischemia–reperfusion injury in the large animal model. First, a reciprocal decrease in Bcl-X_L and increase in Bcl-X_S was observed, suggesting that a shift in mRNA splicing occurs during ischemia–reperfusion injury that favors production of the apoptosis-inducing Bcl-X_S protein. Diminished Bcl-X_L immunoreactivity has also been observed in neurons following middle cerebral artery occlusion in rats (Gillardon et al., 1996b). Bcl-X_L overexpression was shown to protect neurons from injury during brain ischemia in transgenic mice (Parsadianian et al., 1998).

Second, levels of pro-apoptotic Bax and Bak proteins increased following transient global ischemia, though changes in Bak were less obvious by immunoblotting. This is possibly due to the heterogeneity of cell populations that contribute to the protein samples used for immunoblot measurements. These results agree with our prior reports on upregulation of Bax protein levels in neurons following transient ischemic episode in rat focal (Isenmann et al., 1998) and global ischemia (Krajewski et al., 1995), and in the gerbil model of global ischemia (Antonawich et al., 1998).

Third, immunohistochemistry determined that levels of Bcl-2 declined following ischemia–reperfusion injury. Smaller isoforms of Bcl-2 were detected by immunoblotting suggesting caspsase-mediated cleavage of this protein, as reported for in vitro culture models (Cheng et al., 1997). Though only correlative, immunoblot comparisons of the time course of caspsase-3, -6, -10 processing with Bcl-2 cleavage were consistent with the possibility of caspsase-mediated cleavage of Bcl-2. Caspsase cleavage of Bcl-2 at asparatic acid 34 converts this protein from an anti-apoptotic protector to a pro-apoptotic killer (Kirsch et al., 1999).

Fourth, early proteolytic processing of Bid was detected, an event known to activate the latent pro-apoptotic potential of the Bid protein (Gross et al., 1999). The demonstration of cleaved Bid in the brain during ischemia and following reperfusion implies the activation of TNF-family death receptor pathways since activation of caspsase-8 by these cytokine receptors is known to result in cleavage of and activation of Bid. Cleaved Bid then translocates to mitochondria and induces cytochrome *c* release, thus defining an important mechanism for cross-talk between the death receptor and mitochondrial pathways for apoptosis (Gross et al., 1999). In mouse stroke models, the activation of Bid was reported to occur 3 h after ischemia and in a caspsase-8-dependent fashion. Inversely, Bid (–/–) mice were shown to have a significant attenuation of infarction and significantly lower release of cytochrome *c* after

transitory occlusion of the middle cerebral artery (Plesnila et al., 2002).

However, in addition to caspase-8-dependent cleavage of Bid, lysosomal proteases have also been recently shown to generate similar length cleaved fragments of this protein, which are competent to induce cytochrome *c* release from mitochondria (Stoka et al., 2001). Moreover, other investigators have suggested the possibility of cross-talk among the calpain, cathepsin, and caspase protease systems during brain ischemia (Rami et al., 2000; Yamashima, 2000). We have reported previously the cleavage of Bid by calpains during myocardial ischemia/reperfusion (Chen et al., 2001). In the present study, it appears from our Western blot investigation that of all apoptosis proteins analyzed, Bid is the only one to be cleaved early during ischemia, in contrast to mouse model showing late Bid processing during the reperfusion phase (Plesnila et al., 2002). This suggests that Bid is particularly sensitive to calpain or lysosomal protease cleavage. Thus, further studies are required to dissect the mechanisms that account for the Bid cleavage observed after cerebral ischemia–reperfusion injury in our large animal model.

Though much attention is given to mechanisms of neuronal cell death during ischemic process, it is important

to note that besides neurons, astro- and oligodendroglia undergo apoptosis following ischemia–reperfusion injury (Goldberg and Ransom, 2003). Oligodendrocytes, a major cellular component of white matter, are the only myelin-forming cells of the CNS. Therefore, it is essential to protect oligodendrocytes and neurons against ischemic insult. Following transient global ischemia, we observed in some regions of the brain that DNA fragmentation in astroglia and satellite oligodendroglia preceded DNA fragmentation in neurons, implying that the glial cells are highly vulnerable to ischemic damage. This observation agrees with previous reports that suggest glia damage is a very early event (Banati et al., 1996).

In non-ischemic brain, we observed the expression of several caspase proforms in astro- and oligodendrocytes, including caspase-3, -6, -8, -9, and -10, suggesting that these cells possess the proteases required for activation of both the mitochondrial and TNF-family death receptor pathways for apoptosis. Early increases in nuclear caspase-6 immunostaining in astroglia and oligodendroglia, and co-localization of caspase-6 and TUNEL positivity in ischemia-vulnerable regions of the brain that occur before caspase-3 activation may implicate activation of this caspase by

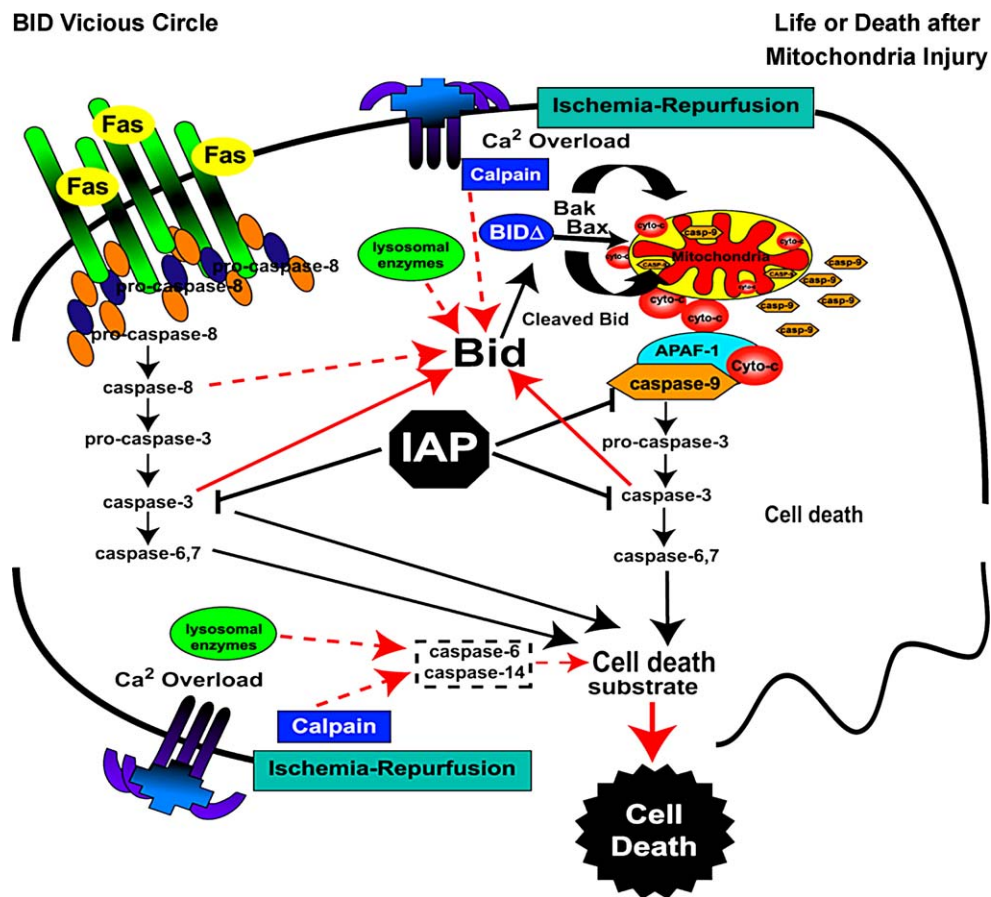


Fig. 7. Graphic summary of events after global brain ischemia during reperfusion. The activation of major, caspase-dependant apoptosis pathways, the possible cross-talk between necrosis inducing cytoplasmic-lysosomal proteases and their possible interaction with Bcl-2 and caspase protein families are depicted. Calcium flux and energy depletion after mitochondria injury is seen as a major reason of the cell collapse either in acute form, resembling necrosis or a delayed form corresponding to an apoptotic type.

mechanisms related to necrosis rather than apoptosis. Later, nuclear immunopositivity for caspase-8 and for processed caspase-3 within affected glial cells was also observed, implying the involvement of a death receptor pathway with Bid processing and a possible cross-talk between JNK and intrinsic cell death pathway in the induction of pronounced apoptotic changes (Deng et al., 2003). This concept is consistent with reports of cytokine activation of these cells during cerebral ischemia (Craighead et al., 2000; Shibata et al., 2000). Altogether, our results indicate that glial cells activate early apoptotic programs during ischemia–reperfusion injury. It remains to be determined to what extent glial cell death indirectly contributes to neuronal death due to loss of trophic factor support, decreased L-glutamate sequestration, or other mechanisms.

In conclusion, rapid, cell-selective processing of apoptosis-regulatory proteins occurs in a clinically relevant model of ischemic brain injury caused by cardiac arrest and resuscitation. A very early cleavage of Bid during ischemia alone and before reperfusion, and a rapid depletion of 32-kDa pro-caspase-14 from the canine hippocampus after induction of ischemia, may be suggestive of the involvement of calpains in the processing of these proteins. Demonstration of Bid cleavage by calpains during myocardial ischemia/reperfusion (Chen et al., 2001), and of *in vitro* cleavage of recombinant mouse caspase-14 by calpain-I in the present study lend support to this assumption.

The chain of events, evoked by oxygen-glucose deprivation and the resultant calcium-ion flux (Lopachin, 1999; LoPachin et al., 2001) in ischemia–reperfusion, is depicted in Fig. 7. These results, taken together with evidence obtained *in vitro* demonstrating close relationships between caspases, calpains, and calpastatin (Neumar et al., 2003; Rami, 2003), justify further *in vivo* exploration of cross-talk between caspase-regulated apoptosis pathways and other protease families during cerebral ischemia. These investigations may provide important insights necessary for devising therapeutic strategies that will provide efficient protection against the cellular damage associated with cerebral ischemic insults.

Acknowledgments

This work was supported by NIH Grant NS36821 (SK), NS34152 (GF), and NS37878 (HS). We wish to thank Steven Banares and Xianshu Huang for technical assistance.

References

Ahmad, M., Srinivasula, S.M., Hegde, R., Mukattash, R., Fernandes-Alnemri, T., Alnemri, E.S., 1998. Identification and characterization of murine caspase-14, a new member of the caspase family. *Cancer Res.* 58, 5201–5205.

Antonawich, F.J., Krajewski, S., Reed, J.C., Davis, J.N., 1998. Bcl-x(l) Bax

interaction after transient global ischemia. *J. Cereb. Blood Flow Metab.* 18, 882–886.

Asahi, M., Hoshimaru, M., Uemura, Y., Tokime, T., Kojima, M., Ohtsuka, T., Matsuura, N., Aoki, T., Shibahara, K., Kikuchi, H., 1997. Expression of interleukin-1 beta converting enzyme gene family and bcl-2 gene family in the rat brain following permanent occlusion of the middle cerebral artery. *J. Cereb. Blood Flow Metab.* 17, 11–18.

Atlante, A., Bobba, A., Calissano, P., Passarella, S., Marra, E., 2003. The apoptosis/necrosis transition in cerebellar granule cells depends on the mutual relationship of the antioxidant and the proteolytic systems which regulate ROS production and cytochrome *c* release en route to death. *J. Neurochem.* 84, 960–971.

Banati, R.B., Gehrman, J., Kreutzberg, G.W., 1996. Early glial reactions in ischemic lesions. *Adv. Neurol.* 71, 329–336 (discussion 336–327).

Bellows, D.S., Chau, B.N., Lee, P., Lazebnik, Y., Burns, W.H., Hardwick, J.M., 2000. Antiapoptotic herpesvirus Bcl-2 homologs escape caspase-mediated conversion to proapoptotic proteins. *J. Virol.* 74, 5024–5031.

Benchoua, A., Guegan, C., Couriaud, C., Hosseini, H., Sampaio, N., Morin, D., Onteniente, B., 2001. Specific caspase pathways are activated in the two stages of cerebral infarction. *J. Neurosci.* 21, 7127–7134.

Boise, L.H., Gonzalez-Garcia, M., Postema, C.E., Ding, L., Lindsten, T., Turka, L.A., Mao, X., Nunez, G., Thompson, C.B., 1993. bcl-x, a bcl-2-related gene that functions as a dominant regulator of apoptotic cell death. *Cell* 74, 597–608.

Cao, G., Minami, M., Pei, W., Yan, C., Chen, D., O'Horo, C., Graham, S.H., Chen, J., 2001. Intracellular Bax translocation after transient cerebral ischemia: implications for a role of the mitochondrial apoptotic signaling pathway in ischemic neuronal death. *J. Cereb. Blood Flow Metab.* 21, 321–333.

Chen, J., Nagayama, T., Jin, K., Stetler, R.A., Zhu, R.L., Graham, S.H., Simon, R.P., 1998. Induction of caspase-3-like protease may mediate delayed neuronal death in the hippocampus after transient cerebral ischemia. *J. Neurosci.* 18, 4914–4928.

Chen, M., He, H., Zhan, S., Krajewski, S., Reed, J.C., Gottlieb, R.A., 2001. Bid is cleaved by calpain to an active fragment *in vitro* and during myocardial ischemia/reperfusion. *J. Biol. Chem.* 276, 30724–30728.

Cheng, E.H., Kirsch, D.G., Clem, R.J., Ravi, R., Kastan, M.B., Bedi, A., Ueno, K., Hardwick, J.M., 1997. Conversion of Bcl-2 to a Bax-like death effector by caspases. *Science* 278, 1966–1968.

Chien, A.J., Presland, R.B., Kuechle, M.K., 2002. Processing of native caspase-14 occurs at an atypical cleavage site in normal epidermal differentiation. *Biochem. Biophys. Res. Commun.* 296, 911–917.

Cho, S., Liu, D., Gonzales, C., Zaleska, M.M., Wood, A., 2003. Temporal assessment of caspase activation in experimental models of focal and global ischemia. *Brain Res.* 982, 146–155.

Cohen, G.M., 1997. Caspases: the executioners of apoptosis. *Biochem. J.* 326 (Pt. 1), 1–16.

Craighead, M., Pole, J., Waters, C., 2000. Caspases mediate C2-ceramide-induced apoptosis of the human oligodendroglial cell line, MO3.13. *Neurosci. Lett.* 278, 125–128.

Darzynkiewicz, Z., Bedner, E., Traganos, F., 2001. Difficulties and pitfalls in analysis of apoptosis. *Methods Cell Biol.* 63, 527–546.

Deng, Y., Ren, X., Yang, L., Lin, Y., Wu, X., 2003. A JNK-dependent pathway is required for TNFalpha-induced apoptosis. *Cell* 115, 61–70.

Endres, M., Namura, S., Shimizu-Sasamata, M., Waerber, C., Zhang, L., Gomez-Isla, T., Hyman, B.T., Moskowitz, M.A., 1998. Attenuation of delayed neuronal death after mild focal ischemia in mice by inhibition of the caspase family. *J. Cereb. Blood Flow Metab.* 18, 238–247.

Erhardt, P., Cooper, G.M., 1996. Activation of the CPP32 apoptotic protease by distinct signaling pathways with differential sensitivity to Bcl-xL. *J. Biol. Chem.* 271, 17601–17604.

Fink, K., Zhu, J., Namura, S., Shimizu-Sasamata, M., Endres, M., Ma, J., Dalkara, T., Yuan, J., Moskowitz, M.A., 1998. Prolonged therapeutic window for ischemic brain damage caused by delayed caspase activation. *J. Cereb. Blood Flow Metab.* 18, 1071–1076.

Forsting, M., Reith, W., Dorfler, A., Meyding-Lamade, U., Sartor, K.,

1994. MRI monitoring of experimental cerebral ischaemia: comparison of two models. *Neuroradiology* 36, 264–268.
- Gillardon, F., Lenz, C., Waschke, K.F., Krajewski, S., Reed, J.C., Zimmermann, M., Kuschinsky, W., 1996a. Altered expression of Bcl-2, Bcl-X, BAX, and c-Fos colocalizes with DNA fragmentation and ischemic cell damage following middle cerebral artery occlusion in rats. *Mol. Brain Res.* 40, 254–260.
- Gillardon, F., Lenz, C., Waschke, K.F., Krajewski, S., Reed, J.C., Zimmermann, M., Kuschinsky, W., 1996b. Altered expression of Bcl-2, Bcl-X, Bax, and c-Fos colocalizes with DNA fragmentation and ischemic cell damage following middle cerebral artery occlusion in rats. *Brain Res. Mol. Brain Res.* 40, 254–260.
- Gillardon, F., Bottiger, B., Schmitz, B., Zimmermann, M., Hossmann, K.A., 1997. Activation of CPP-32 protease in hippocampal neurons following ischemia and epilepsy. *Brain Res. Mol. Brain Res.* 50, 16–22.
- Goldberg, M.P., Ransom, B.R., 2003. New light on white matter. *Stroke* 34, 330–332.
- Green, D.R., Reed, J.C., 1998. Mitochondria and apoptosis. *Science* 281, 1309–1312.
- Gross, A., Yin, X.M., Wang, K., Wei, M.C., Jockel, J., Milliman, C., Erdjument-Bromage, H., Tempst, P., Korsmeyer, S.J., 1999. Caspase cleaved BID targets mitochondria and is required for cytochrome *c* release, while BCL-XL prevents this release but not tumor necrosis factor-R1/Fas death. *J. Biol. Chem.* 274, 1156–1163.
- Himi, T., Ishizaki, Y., Murota, S., 1998. A caspase inhibitor blocks ischaemia-induced delayed neuronal death in the gerbil. *Eur. J. Neurosci.* 10, 777–781.
- Hof, P.R., Vissavajhala, P., Rosenthal, R.E., Fiskum, G., Morrison, J.H., 1996. Distribution of glutamate receptor subunit proteins GluR2(4), GluR5/6/7, and NMDAR1 in the canine and primate cerebral cortex: a comparative immunohistochemical analysis. *Brain Res.* 723, 77–89.
- Hu, S., Snipas, S.J., Vincenz, C., Salvesen, G., Dixit, V.M., 1998. Caspase-14 is a novel developmentally regulated protease. *J. Biol. Chem.* 273, 29648–29653.
- Isenmann, S., Stoll, G., Schroeter, M., Krajewski, S., Reed, J.C., Bahr, M., 1998. Differential regulation of Bax, Bcl-2, and Bcl-X proteins in focal cortical ischemia in the rat. *Brain Pathol.* 8, 49–62 (discussion 62–43).
- Ishisaka, R., Utsumi, T., Yabuki, M., Kanno, T., Furuno, T., Inoue, M., Utsumi, K., 1998. Activation of caspase-3-like protease by digitonin-treated lysosomes. *FEBS Lett.* 435, 233–236.
- Jaeschke, H., Lemasters, J.J., 2003. Apoptosis versus oncotic necrosis in hepatic ischemia/reperfusion injury. *Gastroenterology* 125, 1246–1257.
- Jin, K., Graham, S.H., Mao, X., Nagayama, T., Simon, R.P., Greenberg, D.A., 2001. Fas (CD95) may mediate delayed cell death in hippocampal CA1 sector after global cerebral ischemia. *J. Cereb. Blood Flow Metab.* 21, 1411–1421.
- Kirsch, D.G., Doseff, A., Chau, B.N., Lim, D.S., de Souza-Pinto, N.C., Hansford, R., Kastan, M.B., Lazebnik, Y.A., Hardwick, J.M., 1999. Caspase-3-dependent cleavage of Bcl-2 promotes release of cytochrome *c*. *J. Biol. Chem.* 274, 21155–21161.
- Kluck, R.M., Bossy-Wetzel, E., Green, D.R., Newmeyer, D.D., 1997. The release of cytochrome *c* from mitochondria: a primary site for Bcl-2 regulation of apoptosis. *Science* 275, 1132–1136.
- Korsmeyer, S.J., Wei, M.C., Saito, M., Weiler, S., Oh, K.J., Schlesinger, P.H., 2000. Pro-apoptotic cascade activates BID, which oligomerizes BAK or BAX into pores that result in the release of cytochrome *c*. *Cell Death Differ.* 7, 1166–1173.
- Krajewski, S., Bodrug, S., Gascoyne, R., Berean, K., Krajewska, M., Reed, J.C., 1994a. Immunohistochemical analysis of Mcl-1 and Bcl-2 proteins in normal and neoplastic lymph nodes. *Am. J. Pathol.* 145, 515–525.
- Krajewski, S., Krajewska, M., Shabaik, A., Miyashita, T., Wang, H.G., Reed, J.C., 1994b. Immunohistochemical determination of in vivo distribution of Bax, a dominant inhibitor of Bcl-2. *Am. J. Pathol.* 145, 1323–1336.
- Krajewski, S., Krajewska, M., Shabaik, A., Wang, H.G., Irie, S., Fong, L., Reed, J.C., 1994c. Immunohistochemical analysis of in vivo patterns of Bcl-X expression. *Cancer Res.* 54, 5501–5507.
- Krajewski, S., Mai, J.K., Krajewska, M., Sikorska, M., Mossakowski, M.J., Reed, J.C., 1995. Upregulation of bax protein levels in neurons following cerebral ischemia. *J. Neurosci.* 15, 6364–6376.
- Krajewski, S., Krajewska, M., Reed, J.C., 1996a. Immunohistochemical analysis of in vivo patterns of Bak expression, a proapoptotic member of the Bcl-2 protein family. *Cancer Res.* 56, 2849–2855.
- Krajewski, S., Zapata, J.M., Reed, J.C., 1996b. Detection of multiple antigens on western blots. *Anal. Biochem.* 236, 221–228.
- Krajewska, M., Wang, H.G., Krajewski, S., Zapata, J.M., Shabaik, A., Gascoyne, R., Reed, J.C., 1997. Immunohistochemical analysis of in vivo patterns of expression of CPP32 (Caspase-3), a cell death protease. *Cancer Res.* 57, 1605–1613.
- Krajewski, S., Krajewska, M., Ellerby, L.M., Welsh, K., Xie, Z., Deveraux, Q.L., Salvesen, G.S., Bredesen, D.E., Rosenthal, R.E., Fiskum, G., Reed, J.C., 1999. Release of caspase-9 from mitochondria during neuronal apoptosis and cerebral ischemia. *Proc. Natl. Acad. Sci. U. S. A.* 96, 5752–5757.
- Krajewska, M., Mai, J.K., Zapata, J.M., Ashwell, K.W., Schendel, S.L., Reed, J.C., Krajewski, S., 2002a. Dynamics of expression of apoptosis-regulatory proteins Bid, Bcl-2, Bcl-X, Bax and Bak during development of murine nervous system. *Cell Death Differ.* 9, 145–157.
- Krajewska, M., Zapata, J.M., Meinhold-Heerlein, I., Hedayat, H., Monks, A., Bettendorf, H., Shabaik, A., Bubendorf, L., Kallioniemi, O.P., Kim, H., Reifemberger, G., Reed, J.C., Krajewski, S., 2002b. Expression of Bcl-2 family member Bid in normal and malignant tissues. *Neoplasia* 4, 129–140.
- Krupinski, J., Lopez, E., Marti, E., Ferrer, I., 2000. Expression of caspases and their substrates in the rat model of focal cerebral ischemia. *Neurobiol. Dis.* 7, 332–342.
- Le, D.A., Wu, Y., Huang, Z., Matsushita, K., Plesnila, N., Augustinack, J.C., Hyman, B.T., Yuan, J., Kuida, K., Flavell, R.A., Moskowitz, M.A., 2002. Caspase activation and neuroprotection in caspase-3-deficient mice after in vivo cerebral ischemia and in vitro oxygen glucose deprivation. *Proc. Natl. Acad. Sci. U. S. A.* 99, 15188–15193.
- Li, H., Zhu, H., Xu, C.J., Yuan, J., 1998. Cleavage of BID by caspase 8 mediates the mitochondrial damage in the Fas pathway of apoptosis. *Cell* 94, 491–501.
- Linnik, M.D., Zobrist, R.H., Hatfield, M.D., 1993. Evidence supporting a role for programmed cell death in focal cerebral ischemia in rats. *Stroke* 24, 2002–2008 (discussion 2008–2009).
- Liu, Y., Rosenthal, R.E., Haywood, Y., Miljkovic-Lolic, M., Vanderhoek, J.Y., Fiskum, G., 1998. Normoxic ventilation after cardiac arrest reduces oxidation of brain lipids and improves neurological outcome. *Stroke* 29, 1679–1686.
- Lopachin, R.M., 1999. Intraneuronal ion distribution during experimental oxygen/glucose deprivation. Routes of ion flux as targets of neuroprotective strategies. *Ann. N. Y. Acad. Sci.* 890, 191–203.
- LoPachin, R.M., Gaughan, C.L., Lehning, E.J., Weber, M.L., Taylor, C.P., 2001. Effects of ion channel blockade on the distribution of Na, K, Ca and other elements in oxygen-glucose deprived CA1 hippocampal neurons. *Neuroscience* 103, 971–983.
- Ma, J., Endres, M., Moskowitz, M.A., 1998. Synergistic effects of caspase inhibitors and MK-801 in brain injury after transient focal cerebral ischaemia in mice. *Br. J. Pharmacol.* 124, 756–762.
- Mashima, T., Naito, M., Noguchi, K., Miller, D.K., Nicholson, D.W., Tsuruo, T., 1997. Actin cleavage by CPP-32/apopain during the development of apoptosis. *Oncogene* 14, 1007–1012.
- Matsushita, K., Wu, Y., Qiu, J., Lang-Lazdunski, L., Hirt, L., Waerber, C., Hyman, B.T., Yuan, J., Moskowitz, M.A., 2000. Fas receptor and neuronal cell death after spinal cord ischemia. *J. Neurosci.* 20, 6879–6887.
- Namura, S., Zhu, J., Fink, K., Endres, M., Srinivasan, A., Tomaselli, K.J., Yuan, J., Moskowitz, M.A., 1998. Activation and cleavage of caspase-3 in apoptosis induced by experimental cerebral ischemia. *J. Neurosci.* 18, 3659–3668.
- Neumar, R.W., Xu, Y.A., Gada, H., Guttman, R.P., Siman, R., 2003.

- Cross-talk between calpain and caspase proteolytic systems during neuronal apoptosis. *J. Biol. Chem.* 278, 14162–14167.
- Nicholson, D.W., Thornberry, N.A., 1997. Caspases: killer proteases. *Trends Biochem. Sci.* 22, 299–306.
- Nicholson, D.W., Ali, A., Thornberry, N.A., Vaillancourt, J.P., Ding, C.K., Gallant, M., Gareau, Y., Griffin, P.R., Labelle, M., Lazeznik, Y.A., et al., 1995. Identification and inhibition of the ICE/CED-3 protease necessary for mammalian apoptosis. *Nature* 376, 37–43.
- Nicotera, P., Leist, M., Manzo, L., 1999. Neuronal cell death: a demise with different shapes. *Trends Pharmacol. Sci.* 20, 46–51.
- Niquet, J., Baldwin, R.A., Allen, S.G., Fujikawa, D.G., Wasterlain, C.G., 2003. Hypoxic neuronal necrosis: protein synthesis-independent activation of a cell death program. *Proc. Natl. Acad. Sci. U. S. A.* 100, 2825–2830.
- Nunez, G., Benedict, M.A., Hu, Y., Inohara, N., 1998. Caspases: the proteases of the apoptotic pathway. *Oncogene* 17, 3237–3245.
- O'Brien, S.J., Murphy, W.J., 2003. Genomics. A dog's breakfast? *Science* 301, 1854–1855.
- Onteniente, B., Couriaud, C., Braudeau, J., Benchoua, A., Guegan, C., 2003. The mechanisms of cell death in focal cerebral ischemia highlight neuroprotective perspectives by anti-caspase therapy. *Biochem. Pharmacol.* 66, 1643–1649.
- Parsadanian, A.S., Cheng, Y., Keller-Peck, C.R., Holtzman, D.M., Snider, W.D., 1998. Bcl-xL is an antiapoptotic regulator for postnatal CNS neurons. *J. Neurosci.* 18, 1009–1019.
- Plesnila, N., Zinkel, S., Amin-Hanjani, S., Qiu, J., Korsmeyer, S.J., Moskowitz, M.A., 2002. Function of BID—A molecule of the bcl-2 family—In ischemic cell death in the brain. *Eur. Surg. Res.* 34, 37–41.
- Rami, A., 2003. Ischemic neuronal death in the rat hippocampus: the calpain-calpastatin-caspase hypothesis. *Neurobiol. Dis.* 13, 75–88.
- Rami, A., Agarwal, R., Botez, G., Winckler, J., 2000. mu-Calpain activation, DNA fragmentation, and synergistic effects of caspase and calpain inhibitors in protecting hippocampal neurons from ischemic damage. *Brain Res.* 866, 299–312.
- Rami, A., Jansen, S., Giesser, I., Winckler, J., 2003. Post-ischemic activation of caspase-3 in the rat hippocampus: evidence of an axonal and dendritic localisation. *Neurochem. Int.* 43, 211–223.
- Reed, J.C., 1997. Double identity for proteins of the Bcl-2 family. *Nature* 387, 773–776.
- Resing, K.A., Walsh, K.A., Haugen-Scotfield, J., Dale, B.A., 1989. Identification of proteolytic cleavage sites in the conversion of profilaggrin to filaggrin in mammalian epidermis. *J. Biol. Chem.* 264, 1837–1845.
- Rosenthal, R.E., Hamud, F., Fiskum, G., Varghese, P.J., Sharpe, S., 1987. Cerebral ischemia and reperfusion: prevention of brain mitochondrial injury by lidoflazine. *J. Cereb. Blood Flow Metab.* 7, 752–758.
- Rosenthal, R.E., Silbergleit, R., Hof, P.R., Haywood, Y., Fiskum, G., 2003. Hyperbaric oxygen reduces neuronal death and improves neurological outcome after canine cardiac arrest. *Stroke* 34, 1311–1316.
- Salvesen, G.S., Dixit, V.M., 1997. Caspases: intracellular signaling by proteolysis. *Cell* 91, 443–446.
- Sasaki, C., Kitagawa, H., Zhang, W.R., Warita, H., Sakai, K., Abe, K., 2000. Temporal profile of cytochrome *c* and caspase-3 immunoreactivities and TUNEL staining after permanent middle cerebral artery occlusion in rats. *Neuro. Res.* 22, 223–228.
- Scaffidi, C., Medema, J.P., Krammer, P.H., Peter, M.E., 1997. FLICE is predominantly expressed as two functionally active isoforms, caspase-8/a and caspase-8/b. *J. Biol. Chem.* 272, 26953–26958.
- Sei, Y., Von Lubitz, K.J., Basile, A.S., Borner, M.M., Lin, R.C., Skolnick, P., Fossom, L.H., 1994. Internucleosomal DNA fragmentation in gerbil hippocampus following forebrain ischemia. *Neurosci. Lett.* 171, 179–182.
- Shibata, M., Hisahara, S., Hara, H., Yamawaki, T., Fukuuchi, Y., Yuan, J., Okano, H., Miura, M., 2000. Caspases determine the vulnerability of oligodendrocytes in the ischemic brain. *J. Clin. Invest.* 106, 643–653.
- Snider, B.J., Gottron, F.J., Choi, D.W., 1999. Apoptosis and necrosis in cerebrovascular disease. *Ann. N. Y. Acad. Sci.* 893, 243–253.
- Springer, J.E., Azbill, R.D., Knapp, P.E., 1999. Activation of the caspase-3 apoptotic cascade in traumatic spinal cord injury. *Nat. Med.* 5, 943–946.
- Stegh, A.H., Barnhart, B.C., Volkland, J., Algeciras-Schimnich, A., Ke, N., Reed, J.C., Peter, M.E., 2002. Inactivation of caspase-8 on mitochondria of Bcl-xL-expressing MCF7-Fas cells: role for the bifunctional apoptosis regulator protein. *J. Biol. Chem.* 277, 4351–4360.
- Stoka, V., Turk, B., Schendel, S.L., Kim, T.H., Cirman, T., Snipas, S.J., Ellerby, L.M., Bredesen, D., Freeze, H., Abrahamson, M., Bromme, D., Krajewski, S., Reed, J.C., Yin, X.M., Turk, V., Salvesen, G.S., 2001. Lysosomal protease pathways to apoptosis. Cleavage of bid, not procaspases, is the most likely route. *J. Biol. Chem.* 276, 3149–3157.
- Thornberry, N.A., Lazeznik, Y., 1998. Caspases: enemies within. *Science* 281, 1312–1316.
- Van de Craen, M., Van Loo, G., Pype, S., Van Crieckinge, W., Van den brande, I., Molemans, F., Fiers, W., Declercq, W., Vandenebeele, P., 1998. Identification of a new caspase homologue: caspase-14. *Cell Death Differ.* 5, 838–846.
- Velier, J.J., Ellison, J.A., Kikly, K.K., Spera, P.A., Barone, F.C., Feuerstein, G.Z., 1999. Caspase-8 and caspase-3 are expressed by different populations of cortical neurons undergoing delayed cell death after focal stroke in the rat. *J. Neurosci.* 19, 5932–5941.
- Vogel, P., Putten, H., Popp, E., Krumnikl, J.J., Teschendorf, P., Galmbacher, R., Kisielow, M., Wiessner, C., Schmitz, A., Tomaselli, K.J., Schmitz, B., Martin, E., Bottiger, B.W., 2003. Improved resuscitation after cardiac arrest in rats expressing the baculovirus caspase inhibitor protein p35 in central neurons. *Anesthesiology* 99, 112–121.
- von Mering, M., Wellmer, A., Michel, U., Bunkowski, S., Tlustochowska, A., Bruck, W., Kuhnt, U., Nau, R., 2001. Transcriptional regulation of caspases in experimental pneumococcal meningitis. *Brain Pathol.* 11, 282–295.
- Wang, X., Ryter, S.W., Dai, C., Tang, Z.L., Watkins, S.C., Yin, X.M., Song, R., Choi, A.M., 2003. Necrotic cell death in response to oxidant stress involves the activation of the apoptogenic caspase-8/bid pathway. *J. Biol. Chem.* 278, 29184–29191.
- Yamashima, T., 2000. Implication of cysteine proteases calpain, cathepsin and caspase in ischemic neuronal death of primates. *Prog. Neurobiol.* 62, 273–295.
- Yamashima, T., Saido, T.C., Takita, M., Miyazawa, A., Yamano, J., Miyakawa, A., Nishijyo, H., Yamashita, J., Kawashima, S., Ono, T., Yoshio-ka, T., 1996. Transient brain ischaemia provokes Ca²⁺, PIP₂ and calpain responses prior to delayed neuronal death in monkeys. *Eur. J. Neurosci.* 8, 1932–1944.
- Yang, J., Liu, X., Bhalla, K., Kim, C.N., Ibrado, A.M., Cai, J., Peng, T.I., Jones, D.P., Wang, X., 1997. Prevention of apoptosis by Bcl-2: release of cytochrome *c* from mitochondria blocked. *Science* 275, 1129–1132.
- Yuan, J., 1997. Transducing signals of life and death. *Curr. Opin. Cell Biol.* 9, 247–251.
- Zulch, K.J., Gessaga, E., 1972. Infarcts in the carotid system. *Vasc. Surg.* 6, 114–119.